SEMMELWEIS EGYETEM

DOKTORI ISKOLA

Ph.D. értekezések

3463.

SAMANEH HAGHIGHI

Kórélettan és transzlációs medicina

című program

Programvezető: Dr. Zsembery Ákos, egyetemi docen

Témavezető: Dr. Kökény Gábor, habilitált egyetemi docens

MOLECULAR BACKGROUND OF NSAID INDUCED RENAL AND INTESTINAL DAMAGE

PhD thesis

Samaneh Haghighi

Semmelweis University Doctoral College

Theoretical and Translational Medicine Division

Supervisor: Gábor Kökény, MD, PhD

Official reviewers: Balázs Sági, MD, Ph.D
Sára Zsigrai, MD, Ph.D

Head of the Complex Examination Committee: Alán Alpár, DSc

Members of the Complex Examination Committee: Cervenák László, Ph.D
Tóth Miklós, DSc

Budapest
2026

TABLE OF CONTENTS

List of Abbreviations

ACTA2: Alpha smooth muscle actin

AKT: Protein Kinase B

AMPs: Antimicrobial peptides

ATG5: Autophagy related 5

ATG7: Autophagy related 7

BECN1: Beclin 1

Camp: Cathelicidin antimicrobial peptide

CEL: Celecoxib

CKD: Chronic kidney disease

CLU: Clusterin

COL1A1: Collagen type I alpha 1 chain

COX-1: Cyclooxygenase-1

COX-2: Cyclooxygenase-2

COX2: Cyclooxygenase 2

DAPI: 4',6-diamidino-2-phenylindole

Defa5: Alpha-defensin 5

Defb2: Beta-defensin 2

DMEM: Dulbecco's Modified Eagle Medium

ECM: Extracellular matrix

EGR1: Early growth response 1

EGR2: Early growth response 2

EMT: Epithelial-to-mesenchymal transition

FBS: Fetal bovine serum

FOS: FOS proto-oncogene, AP-1 transcription factor subunit

GAPDH: Glyceraldehyde-3-phosphate dehydrogenase

GFR: Glomerular filtration rate

H&E: Hematoxylin and eosin

HEqD: Human equivalent doses

HIF1A: Hypoxia-inducible factor 1 alpha

HMOX1: Heme oxygenase 1

HO-1: Heme oxygenase-1

IL10: Interleukin 10

IL1B: Interleukin 1 beta

IND: Indomethacin

JUN: Jun proto-oncogene, AP-1 transcription factor subunit

KSFM: Keratinocyte Serum-Free Medium

LC3: Microtubule-associated protein 1 light chain 3

LC3A: Microtubule-associated protein 1 light chain 3 alpha

LCN2: Lipocalin 2

LGALS3: Galectin 3

MMP9: Matrix metalloproteinase 9

MMPs: Matrix metalloproteinases

MPO: Myeloperoxidase

MTT: 3-(4,5-dimethylthiazol-2-yl)-2,5-diphenyltetrazolium bromide

NAP: Naproxen

NF-κB: Nuclear factor kappa B

NGAL: Neutrophil gelatinase-associated lipocalin

NSAIDs: Nonsteroidal anti-inflammatory drugs

pAKT: Phosphorylated AKT

PI3K/Akt: Phosphatidylinositol 3-kinase/Akt

PTX3: Pentraxin 3

PTECs: Proximal tubular epithelial cells

qRT-PCR: Quantitative real-time polymerase chain reaction

ROS: Reactive oxygen species

SQSTM1/p62: Sequestosome 1/p62

TGF-β: Transforming growth factor-beta

TGF-β1: Transforming growth factor-beta 1

TIMP1: Tissue inhibitor of metalloproteinase 1

TIMPs: Tissue inhibitors of metalloproteinases

TNF: Tumor necrosis factor

TNFα: Tumor necrosis factor alpha

α-SMA: Alpha smooth muscle actin

1 INTRODUCTION

1.1 Overview of Nonsteroidal Anti-Inflammatory Drugs (NSAIDs)

Nonsteroidal anti-inflammatory drugs (NSAIDs) hold a prominent position globally among prescription and over-the-counter medications. They are often used to treat pain and inflammatory conditions, including osteoarthritis, rheumatoid arthritis, musculoskeletal pain, and postoperative pain (1, 2). About 30 million people use NSAIDs each day in total. Ibuprofen, diclofenac, and naproxen account for most NSAID use (3).

The pharmacological effects of NSAIDs occur mostly through inhibition of cyclooxygenases, specifically the constitutive enzymes COX-1 and COX-2. These enzymes convert arachidonic acid into prostaglandins, prostacyclin and thromboxane (4, 5). The anti-inflammatory effects and the analgesic effects are attributed mainly to the inhibition of COX-2. Inhibition of COX-1 products also impairs some of the physiological protective functions within the gastrointestinal tract and kidneys (6, 7).

NSAIDs are effective and safe for short-term use. However, high doses or prolonged use are associated with meaningful adverse events in multiple systems. Although upper gastrointestinal tract events are the best-known adverse effects of NSAIDs, the kidney and small intestine are also sites of clinically important NSAID side effects (8). In the kidney, repeated or prolonged use of NSAIDs can lead to hemodynamic acute kidney injury in addition to chronic tubulointerstitial damage (9, 10). Long-term NSAID therapy can cause small intestinal mucosal injury in 50-70% of NSAID users. Most injuries do not show symptoms in the early stages (11).

1.2 NSAID-Induced Renal Fibrosis

Prostaglandins are physiologically critical for regulating renal blood flow, the secretion of renin, and the transport of ions and water within the kidney's tubules (12, 13). Prolonged or high-dose exposure to NSAIDs commonly leads to decreased glomerular filtration rate, impaired renal perfusion, and electrolyte imbalance, particularly in patients with underlying chronic kidney disease (CKD) (14). Consequently, repeated NSAID administration frequently results in progressive tubulointerstitial fibrosis characterized by excessive extracellular matrix accumulation and irreversible loss of renal function (15, 16).

Renal fibrosis is the final common pathway of progressive CKD regardless of the etiology and is characterized by fibroblast activation, tubulointerstitial inflammation, extracellular matrix (ECM) deposition, tubular atrophy, glomerulosclerosis, and microvascular rarefaction (17, 18). Proximal

tubular epithelial cells (PTECs) are especially vulnerable due to their high metabolic demand, abundant mitochondria, and dense apical brush border, which is required for the reabsorption of most of the filtered load (19). Chronic insults trigger maladaptive responses in PTECs, including partial epithelial-to-mesenchymal transition (EMT) and secretion of pro-fibrotic mediators, ultimately driving scar formation (20).

The immortalized human proximal tubular epithelial cell line HK-2 is a reliable tool to investigate these processes in vitro (20).

1.3 TGF-β Signaling in NSAID-Induced Renal Fibrosis

NSAID-induced renal fibrosis is a complex process, in which TGF-β is one of the most important mediators. TGF-β activates canonical (Smad) and non-canonical (non-Smad) signaling pathways and is the key mediator of renal fibrosis in CKD. The TGF-β1 isoform binds to TGF-β type II receptors (TGFBR2), which recruit TGF-β type I receptors (TGFBR1) to activate intracellular pathways responsible for kidney fibrosis (21). TGF-β1 increases ECM deposition, leading to matrix accumulation by enhancing the synthesis of collagen and fibronectin, and by upregulating TIMPs that inhibit MMPs — enzymes that cleave ECM components (22). TGF-β1 also induces EMT, by activating myofibroblasts, leading to scar formation, while causing apoptosis in tubular epithelial cells (23, 24). Targeting TGF-β1 is problematic due to its essential non-fibrotic roles, such as immune regulation, but elucidating its role in renal fibrosis is crucial for CKD therapies (22, 25).

1.4 Role of Early Growth Response Factors in Renal Fibrosis

Early growth response-1 (EGR1, also known as KROX-24), a zinc finger transcription factor, is involved in renal fibrosis, a characteristic feature of chronic kidney disease (CKD) (26). The family of early response genes is characterized by low or undetectable levels in resting cells and can be induced by cytokines, growth factors, hypoxia, or mechanical injury (27, 28).

EGR1 acts as a key transcription factor in the progression of renal fibrosis, primarily by orchestrating pro-fibrotic responses such as upregulation of extracellular matrix (ECM) components, facilitation of epithelial-mesenchymal transition (EMT), and modulation of inflammatory pathways. Evidence indicates that EGR1 plays a crucial role in the development of tubulointerstitial fibrosis. It promotes fibrotic pathways, which leads to an increase in collagen production, a key component of the fibrotic matrix. EGR1 also promotes the transdifferentiation of epithelial cells into myofibroblasts that play a crucial role in the subsequent scarring of the tissue

(29, 30). EGR1 interacts with transforming growth factor-beta (TGF-β), enhancing tissue remodeling through a positive feedback mechanism (26). EGR1 is absent in normal adult kidneys under physiological conditions, although it is present during kidney development. However, EGR1 is rapidly induced in renal tubular epithelial cells following acute or chronic kidney injury, where it contributes to fibrotic processes through multiple mechanisms, including promotion of mesangial cell proliferation, activation of the TGF-β signaling pathway, and induction of transdifferentiation in tubular epithelial cells into mesenchymal-like cells (31-35) . Better understanding the regulation of EGR1, may improve future clinical strategies aimed at reducing tubulointerstitial fibrosis and slowing CKD progression (36).

1.5 NSAIDs and Oxidative Stress

Oxidative stress is an overproduction of reactive oxygen species (ROS), leading to critical damage to the kidney cells (37). The proximal tubule cells are the most affected, where mitochondrial damage occurs. NSAIDs induce the generation of ROS by disrupting the mitochondrial electron transport chain, leading to cell injury and the activation of stress response pathways (38). The stress-inducible heme oxygenase-1 (HMOX1) is upregulated in response to oxidative stress and its expression is significantly increased in renal cells following NSAID treatment. HMOX1 is a marker of cell injury, as its induction is part of the primary response of cells to the harmful effects of ROS, and HMOX1 also generates antioxidant products, biliverdin and carbon monoxide (39, 40). There is also evidence that celecoxib may also induce HMOX1 expression outside the kidney via a ROS-dependent mechanism (40).

Other pathways involved in NSAID-induced oxidative stress include the phosphatidylinositol 3-kinase/Akt (PI3K/Akt) pathway, which is also activated via ROS and is involved in cell survival and inflammation (41). Additionally, celecoxib (a COX-2 inhibitor) may phosphorylate Akt in renal proximal tubular epithelial cells, activating downstream molecules, such as the transcription factor NF-κB, and pro-inflammatory cytokines (40, 42). Understanding the mechanisms that cause oxidative stress is crucial to elucidating the mechanisms underlying NSAID nephrotoxicity.

1.6 Autophagy dysfunction in renal fibrosis

Autophagy is a critical function that enables the cells to maintain their functional, structural, and metabolic homeostasis by degrading and recycling damaged cellular components (43). Autophagy is therefore essential in a healthy kidney. However, autophagy becomes less active during ageing ,

making the kidney more prone to chronic diseases (43). In cases of acute kidney injury, autophagy is usually activated as a defensive response. It is effective in repairing tubular cells by clearing the cells of debris and harmful substances. However, a decline in autophagy during the transition from AKI to chronic kidney disease (CKD) promotes maladaptive repair and progression to tubulointerstitial fibrosis, a hallmark of CKD (44, 45).

TGF-β1 has a dual effect on autophagy of renal tubular epithelial cells. On the one hand, it can stimulate autophagy and increase the formation of autophagosomes by activating genes such as autophagy-related 5 (Atg5), autophagy-related 7 (Atg7), microtubule-associated protein 1 light chain 3 (LC3), and Beclin-1 (46, 47). The formation of autophagosomes is accompanied by the appearance of LC3-II on the autophagosome membrane and seems to be cytoprotective at an early stage. However, continuous TGF-β signaling can also cause fibrosis (48) the effects of which are likely counteracted by autophagy, suppressing the production of mature TGF-β1 within tubular cells (49). Elevated LC3-II or reduced SQSTM1 (p62) levels—a protein degraded during autophagy—indicate robust autophagic activity, while elevated LC3-I and p62 reflect induced autophagy with disrupted clearance (48). As the exact role of autophagy in tubulointerstitial fibrosis remains unclear, and may vary across cell type and microenvironment, further studies should be conducted to elucidate how modulation of autophagy may improve therapeutic approaches for chronic kidney disease.

1.7 NSAID-Induced Small Intestinal Damage: Role of Antimicrobial Peptides and Systemic Effects

NSAID enteropathy represents a significant clinical challenge in patients requiring long-term therapy, characterized by damage to the small intestinal mucosa that often remains asymptomatic in its early phases (50-52). This condition affects a substantial proportion of chronic NSAID users, leading to erosions, ulcers, increased permeability, and chronic inflammation in the small intestine (53, 54). The pathomechanisms of intestinal inflammation in enteropathy include direct mucosal epithelial effects and indirect effects of dysbiosis in the gut microbiota and disruption of host-microbiota interactions, which damage the mucosal barrier and perpetuate immune activation (55, 56), leading to chronic tissue injury and impaired tissue regeneration.

Antimicrobial peptides (AMPs) secreted by Paneth and epithelial cells maintain the homeostasis with commensal bacteria by limiting their penetration from the intestinal lumen and modulating inflammatory response (57). Alterations in AMP expression or function can amplify microbial

imbalances and perpetuate inflammatory cycles during enteropathy. Additionally, the systemic impact of small intestinal injury is reflected in hematological alterations, providing indirect markers of the underlying inflammatory and compensatory processes (58).

2 OBJECTIVES

NSAIDs are widely used analgesics, but their effects on renal tubular epithelial cells, particularly with respect to autophagy, oxidative stress, and pro-fibrotic transcription factors, are poorly understood. NSAID enteropathy may also develop as a side effect of extended NSAID treatment, but the role of intestinal antimicrobial peptides in NSAID enteropathy is unclear.

1. Here, we investigated the effects of NSAIDs on renal tubular cells (*in vitro*) and rat kidneys (*in vivo*) with the following aims:
   - To determine the most suitable cell culture medium formulation for reliable investigation of TGF-β1-induced EMT and NSAID-mediated fibrotic pathways in HK-2 cells.
   - To examine the effects of celecoxib (CEL) and naproxen (NAP), compared to indomethacin (IND), on the expression of fibrosis-related genes and transcription factors in HK-2, murine inner medullary collecting duct (IMCD) cells and the renal medulla of rats.
   - To assess the effects of NSAIDs on autophagy markers, oxidative stress, and survival pathway activation in HK-2 and IMCD cells and rat renal medulla.
   - To investigate which molecular pathways affected by NSAIDs are linked to COX by analyzing the expression of JUN and FOS genes in HK-2, IMCD cells, and rat renal medulla.
   - To investigate the effects of NSAIDs on EGR1 protein expression in vitro and in vivo.
2. To investigate the effects of NSAIDs on the small intestinal mucosal defense and systemic inflammatory markers, we studied the in vivo effects of indomethacin (IND) treatment in rats with the following aims:
   - To determine the time and dose-dependent effects of acute and chronic IND administration on the mRNA expression of the major antimicrobial peptides in the rat small intestinal mucosa.
   - To assess systemic hematological parameters in IND-treated rats as indicators of inflammatory and broader physiological impact of NSAID enteropathy.

3 MATERIALS AND METHODS

3.1 In vitro and in vivo experiments

3.1.1 Culture of HK-2 Cells

HK-2 cells, a human proximal tubule epithelial line (ATCC #CRL-2190), were maintained in a humidified atmosphere of 5% CO_2 at 37°C. Growth was supported using Dulbecco's Modified Eagle Medium (DMEM) containing 5% (v/v) fetal bovine serum (FBS), penicillin (50 U/mL), and streptomycin (50 µg/mL). The culture medium was refreshed every two to three days. Cells were harvested via trypsinization for subculturing or experimental use when they reached 70–80% confluence, which typically occurred within 3–5 days of seeding.

3.1.2 Culture of mIMCD-3 Cells

The murine inner medullary collecting duct cell line mIMCD-3 (American Type Culture Collection (ATCC) #CRL-2123) was incubated under standard conditions (37°C, 5% CO_2). These cells were cultured in low-glucose (1 g/L) DMEM supplemented with 10% (v/v) FBS, 4 mM glutamine, penicillin (100 IU/mL), and streptomycin (100 µg/mL). Regular medium changes were performed to ensure optimal cell growth and viability throughout the culture period.

3.1.3 HK-2 cell culture in different growth media and TGF-β1 stimulation

HK-2 cells (ATCC CRL-2190) were exposed to one of four different culture media conditions (Table 1). The experimental conditions were performed using either cells plated in 6-well plates (1×10^5 cells/well) or in 24-well plates (3×10^4 cells/well) under various media conditions. After overnight incubation, the cells were starved. Cells cultured in the serum-free KSFM were not serum-starved. The other cells were cultured in DMEM/F-12 containing 0.5% FBS for 24 hours and then treated with TGF-β1 or vehicle for an additional 24 hours. Cells were either harvested for RNA isolation using TRIzol reagent (Invitrogen) or proteins were extracted in ice-cold RIPA buffer.

3.1.4 HK-2 and IMCD Cell Culture Treated with Indomethacin, Celecoxib, and Naproxen

HK-2 cells (passages 6–8) and IMCD cells (passages 8–10) were seeded at densities of 3×10^4 and 4×10^4 cells per well, respectively, in 24-well plates. The next day, the medium was changed to Dulbecco's Modified Eagle Medium (DMEM) without serum. Cells were then treated with indomethacin (IND; 20 µg/mL, serving as the reference treatment), celecoxib (CEL; 0.72, 2.1, 4.3, 8.7 µg/mL), or naproxen (NAP; 15, 30, 60, 110 µg/mL), all dissolved in 0.4% dimethyl sulfoxide (DMSO). Control groups received 0.4% DMSO alone. The concentrations were calculated based

on peak plasma concentrations (Cmax) reported in earlier in vivo research (59-61), adjusted for in vitro conditions to confirm therapeutic relevance and prevent cytotoxicity. Concentrations were selected to span a range around the Cmax values, maintaining biologically relevant doses. All treatments were applied for 24 hours (n=6 per group).

Table 1. Cell culture media and their formulation

Medium abbreviations	Formulation
DMEM 5%	The DMEM 5% medium was formulated using Dulbecco's Modified Eagle Medium (DMEM) as a base, which contained 1000 mg/L glucose, L-glutamine, and sodium bicarbonate. This basal medium was then supplemented with 5% (v/v) fetal bovine serum (FBS) and a penicillin-streptomycin antibiotic mixture at final concentrations of 50 U/mL and 50 µg/mL, respectively.
DMEM 10%	The DMEM 10% medium consisted of DMEM supplemented with 1000 mg/L glucose, L-glutamine, sodium bicarbonate, 10% v/v fetal bovine serum, 50 U/mL penicillin, and 50 µg/mL streptomycin.
DMEM F12 10%	DMEM F12 10% medium was made by mixing DMEM and Ham's F12 base media (1:1), adding L-glutamine, 15 mM HEPES buffer, and sodium bicarbonate, and finally adding 10% (v/v) fetal bovine serum FBS plus antibiotics (50 U/mL penicillin and 50 µg/mL streptomycin).
KSFM	The KSFM, or Keratinocyte Serum-Free Medium, was a defined, serum-free formulation. It was specifically supplemented with 0.05 mg/mL of bovine pituitary extract, 5 ng/mL of human recombinant epidermal growth factor, and the standard antibiotic concentrations of 50 U/mL penicillin and 50 µg/mL streptomycin.

3.1.5 Animal experiments

All experimental procedures involving animals were conducted in accordance with Directive 2010/63/EU and received formal approval from the National Scientific Ethical Committee on Animal Experimentation. The specific authorization (PE/EA/1118-6/2020) was granted by the

Food Chain Safety and Animal Health Directorate of the Government Office for Pest County. For this study, male Wistar rats, aged 8–10 weeks (body weight: 180–220 g), were obtained from Toxi-Coop Ltd. (Budapest, Hungary). The animals were housed under standard laboratory conditions, including a constant ambient temperature of 22 ± 2°C and a 12-hour light/dark cycle with a regulated schedule. Throughout the acclimatization and experimental periods, rats had ad libitum access to standard rodent feed and drinking water.

3.1.6 In vivo experimental design for NSAID-Induced Renal Damage

To investigate the chronic renal effects of nonsteroidal anti-inflammatory drugs (NSAIDs), a rodent model was employed using male Wistar rats. The animals were randomly assigned to one of six experimental groups (n=8 per group). The treatment regimen consisted of oral gavage twice daily for 14 days. The administered compounds included celecoxib (CEL) at doses of 10 or 30 mg/kg, naproxen (NAP) at 10 or 20 mg/kg, and a vehicle control (1% hydroxyethylcellulose). An additional group received indomethacin (IND; 2 mg/kg) as a reference COX-1/COX-2 inhibitor. Human equivalent doses (HEqD) were determined using the Reagan-Shaw formula to contextualize the dosing regimen. (62) The calculated HEqDs fell within the range of standard clinical doses: 97 and 292 mg for the CEL doses, 97 and 194 mg for the NAP doses, and 19 mg for the IND dose.

The group receiving the higher dose of NAP (20 mg/kg) exhibited significant health deterioration, necessitating euthanasia of remaining survivors on day 8. At the predefined endpoint of the study, all animals were euthanized via CO_2 asphyxiation. Both kidneys were immediately collected post-mortem. The left kidney was sectioned and preserved in 4% buffered formalin for histological assessment. The right kidney was dissected to separate the cortical and medullary regions; these tissues were then minced and rapidly frozen in liquid nitrogen for subsequent molecular analysis.

3.1.7 In vivo experimental design for NSAID-Induced Enteropathy

Two sequential animal studies were conducted to assess the effects of indomethacin on the levels of the antimicrobial peptides (AMPs) within the intestines. Rats were co-housed to standardize gut microbiota. They were then randomly assigned to either a vehicle (1% hydroxyethylcellulose) or an indomethacin (IND) treatment group.

The first study was designed to characterize the time course of intestinal AMPs expression in a model of acute drug-induced enteropathy. The protocol stated that the IND was administered as a

single 20 mg/kg oral dose. The rats (n = 8 at each time point) were sacrificed at 6, 12, 24, 48, and 72 hours after administration. Control rats had a stable gut microbiota composition under the same environmental conditions at baseline. Therefore, vehicle-treated control animals were sacrificed at the 72-hour time point alone.

In the second experiment, constant administration of low-dose IND was tested. Rats were given 2 mg/kg twice daily for 14 days, or 4 mg/kg twice daily for 7 days. This was based on pilot studies showing moderate enteropathy with the longer duration 4 mg/kg/day dose. However, in the present protocol, the twice daily 4 mg/kg dose led to much more severe enteropathy, in fact, requiring animals to be euthanized one day sooner on account of poor condition than in the original protocol. For the first study, appropriate controls were sacrificed after 2 weeks of treatment with the vehicle, and blood was collected. The small intestine was removed and frozen in liquid nitrogen, then stored at -80 °C until molecular analysis was carried out.

3.2 Hematological Analysis

Vacuette K3 EDTA tubes from Greiner Bio-One, Kremsmünster, Austria, were used to hold the whole-blood samples from rats. The desired hematological parameters were measured using a Sysmex XN-1000 hematological analyzer (Sysmex America, Lincolnshire, IL, USA), in accordance with standard laboratory procedures. The data were automatically calculated by the Sysmex XN-1000 software.

3.3 Quantitative Real-Time PCR Analysis

The Trizol reagent from Invitrogen, Thermo Fisher Scientific, Waltham, MA, USA extracted RNA following the manufacturer's instructions. RNA concentration and quality were determined by using a NanoDrop (ND-2000) spectrophotometer (Thermo Fisher Scientific). cDNA was synthesized by using High-Capacity cDNA Reverse Transcription Kit (Applied Biosystems, Life Technologies, Carlsbad, CA, USA). Quantitative PCR was performed in duplicates. The process occurred on Bio-Rad CFX thermal cycler using SensiFast SYBR Green PCR Master Mix and gene-specific primers. The thermal cycler is from Bio-Rad, Hungary. The master mix is from Bioline, Germany. Reaction specificity and efficiency were confirmed using melting curve analysis. Glyceraldehyde-3-phosphate dehydrogenase (GAPDH) normalized the expression levels. The data were calculated according to the $2^{-\Delta\Delta Ct}$ method as a fold change relative to a reference sample of sorts. All values are given as mean ± SD. In all PCR experiments, positive and negative controls

were run to confirm test specificity and avoid false positive results caused by contamination. Human and Rat primers are detailed in corresponding publications (55, 63, 64).

3.4 Immunoblot

For protein analysis, cellular lysates were prepared from HK-2 and IMCD cell lines using cold denaturing lysis buffers, including RIPA and Laemmli buffers supplemented with β-mercaptoethanol. Tissue samples from the rat kidney medulla (approximately 3 mm^3) were homogenized in ice-cold RIPA lysis buffer. The total protein concentration of all lysates was quantified with a bicinchoninic acid (BCA) assay (Thermo Fisher Scientific, Waltham, MA, USA). For immunoblotting, standardized amounts of protein (20 µg for cell lysates, 60 µg for tissue homogenates) were prepared in Laemmli buffer (Bio-Rad, Hercules, CA, USA). Protein separation was achieved via electrophoresis on 8% or 12% SDS-polyacrylamide gels, followed by transfer onto nitrocellulose membranes using a standard wet transfer system.

Following blocking with 5% non-fat dry milk in Tris-buffered saline and 0.1% Tween 20 (TBST), the membranes were incubated at 4 degrees Celsius overnight with the appropriate primary antibodies. The primary antibodies used in the study have been listed in the corresponding publications (64) . After several washes with TBST, the blots were incubated for 1 hour at room temperature with the appropriate HRP-conjugated secondary antibodies. An ECL substrate detection kit from Thermo Fisher Scientific of Waltham, MA, USA, was applied to the proteins of interest. Protein loading was confirmed through normalizing against tubulin or glyceraldehyde-3-phosphate dehydrogenase (GAPDH). Densitometry comparisons utilized the LI-COR Biosciences (Lincoln, NE, USA) Image Studio Lite software, version 5.2, for analysis.

3.5 MTT Cytotoxicity Assay

For measuring the effect of NSAIDs on cell viability, the MTT assay was used. We seeded HK-2 and IMCD cells at 10,000 cells per well in 96-well plates and incubated them overnight in complete growth medium. Following this incubation, the medium was removed and replaced with 200 µL of serum-free medium containing the respective nonsteroidal anti-inflammatory drug (NSAID) treatments for 24 hours. For measuring the effect of NSAIDs on cell viability, the MTT assay was used. We seeded HK-2 and IMCD cells at 10,000 cells per well in 96-well plates and incubated them overnight in complete growth medium. Someone replaced the growth medium with 200 µL

of serum-free medium that contained the provided nonsteroidal anti-inflammatory drug (NSAID) after 24 hours.

Then, the experimenters removed the medium and added 100 µL of 0.5 mg/mL MTT (3-(4,5-dimethylthiazol-2-yl)-2,5-diphenyltetrazolium bromide) solution afterward. The 96-well plates were returned to the incubator (37°C, 5% CO2) for 2 hours, as the tetrazolium salt reduces to an insoluble product (formazan crystals). Cells were then washed in phosphate-buffered saline (PBS). The dissolved formazan crystals were removed with a pipette, and 100 µL dimethyl sulfoxide (DMSO) was added to the wells to dissolve any remaining formazan crystals. The plates were shaken to ensure the dissolved formazan was mixed throughout the DMSO in each well. The absorbance of each well was measured using a microplate reader (Victor Wallac, PerkinElmer, Waltham, MA, USA) with primary and secondary reference wavelengths of 570 nm and 690 nm, respectively, for background interference. The percentage of cytotoxicity was calculated using the formula % Cytotoxicity = [(Abs_control − Abs_sample)/Abs_control] × 100, where Abs_control and Abs_sample were the mean absorbance of the control and sample group, respectively.

3.6 Immunocytochemistry

For immunocytochemical studies, HK-2 cells (15,000/well) were plated in 8-well chamber slides (Lab-Tek Permanox), treated with IND (40 µg/mL), CEL (2.1 or 8.7 µg/mL), or NAP (30 or 110 µg/mL) for 24 hours, or vehicle control, and analyzed by the immunocytochemical technique described earlier. Another set of cells, treated with 10 ng/mL TGF-β and used as a positive control, was fixed in 4% paraformaldehyde for 15 minutes before staining. Subsequently, cells were permeabilized with 0.25% Triton X-100 for 10 minutes and blocked with 2% donkey serum in 0.1% Tween 20 in phosphate-buffered saline (PBS-T). For immunolabeling, cells were incubated overnight at 4°C with primary antibodies diluted in PBS-T containing 2% goat serum. The primary antibodies used were a rabbit polyclonal anti-EGR1 antibody (Proteintech; 1:200 dilution) and a mouse monoclonal anti-α-SMA (ACTA2) antibody (Sigma-Aldrich; 1:400 dilution) (64).

The following day, after washing, the cells were incubated for 2 hours at room temperature with fluorophore-conjugated secondary antibodies: donkey anti-rabbit IgG conjugated to Alexa Fluor 594 (for EGR1 detection) and donkey anti-mouse IgG conjugated to Alexa Fluor 488 (for α-SMA detection), both used at a 1:200 dilution (Jackson ImmunoResearch). All incubation steps with fluorescent antibodies were performed in the dark. Finally, the slides were washed, mounted with

ProLong Gold antifade reagent containing DAPI (Molecular Probes, Thermo Fisher Scientific), and prepared for imaging.

3.7 Kidney Histology and Immunohistochemistry

Histological assessment of renal injury was performed on kidney tissue samples that had been fixed in formalin and embedded in paraffin. To evaluate tubulointerstitial fibrosis and damage, tissue sections were subjected to Masson's trichrome staining. A blinded, semi-quantitative analysis was conducted under 100x magnification, employing a previously validated scoring system (62). H&E-stained sections were assessed according to a scoring system where a score of 0 indicated normal histology, and scores 1-4 were based on tubular dilation, tubular atrophy, and interstitial mononuclear cell infiltration. Each histological change in an overall view field was scored as 1 point. The arithmetic mean of each score per field was calculated to give the final score for each animal.

Immunohistochemistry for staining EGR1 protein in paraffin-embedded kidney sections utilized heat-induced antigen retrieval (pH 6.0) in citric acid buffer, a standard protocol for such sections. To prevent nonspecific binding, sections were incubated in 5% normal goat serum, followed by an overnight incubation at 4°C with an anti-EGR1 primary antibody (65). A biotinylated goat anti-rabbit secondary antibody was applied for one hour the following day, followed by alkaline phosphatase-streptavidin conjugate detection and chromogen development with Vulcan Fast Red (Biocare Medical). EGR1 immunostaining was evaluated through two blinded methods. First, staining intensity was graded semi-quantitatively on a scale from 0 (absent) to 4 (very intense) at 400x magnification. Second, a quantitative analysis was performed by counting EGR1-positive nuclei in multiple high-power fields (400x), with results expressed as the average number of positive cells per field.

3.8 Data Analysis

Experimental data are presented as mean ± SD. Statistical analysis was performed using IBM SPSS Statistics for Windows, Version 28.0 (Armonk, NY: IBM Corp.). The Shapiro-Wilk test was used to assess data normality. For EMT experiments in HK-2 cells, comparisons were conducted using the Mann-Whitney U test or Kruskal-Wallis test followed by Dunn’s post-hoc where appropriate. Spearman or Pearson’s correlation was applied to examine relationships between ordinal or continuous variables, respectively. For NSAID effects on renal fibrosis and autophagy in HK-2,

mIMCD-3 cells, and rat models (including gene expression and immunoblot), one-way ANOVA followed by Holm–Sidak post-hoc tests was used. For histological scoring in rat kidneys, the Kruskal-Wallis test with Dunn's post-hoc test was employed. In enteropathy studies, one-way ANOVA followed by Holm–Sidak post-hoc test was used for antimicrobial peptide expression and hematological parameters. Spearman's correlation with Benjamini–Hochberg false discovery rate correction was applied for associations in the acute model. Statistical significance was set at $p < 0.05$ (95% confidence level).

4 RESULTS

4.1 NSAID-Induced Renal Damage

4.1.1 Selection of optimal cell culture medium to study HK-2 cells

In order to select the best-suited cell culture medium for NSAID treatment experiments on HK-2 cells, we compared the effects of TGF-β1 (10 ng/ml, 24 h) in four culture media (DMEM 5%, DMEM 10%, DMEM/F12 10% and KSFM) using the results of our previous study (63) .The focus was on EMT-related genes to assess stability and reliability for modeling renal tubular injury.

TGFB1 mRNA was significantly upregulated by TGF-β1 in all media, but changes in *EGR1* mRNA were formulation-dependent (Table 2). Correlation analyses between *TGFB1* and *EGR1* mRNA expression demonstrated the strongest positive relationship in DMEM 5% FBS and a moderate correlation in DMEM/F12 10% FBS, while the other two media showed weak or no correlation (Fig. 1).

Table 2. TGFB1 and EGR1 mRNA levels in HK-2 cells in various media.

TGFB1 expression (n=6-12/group)								
	DMEM 5% CTL	**DMEM 5% TGFb**	**DMEM 10% CTL**	**DMEM 10% TGFb**	**F12 10% CTL**	**F12 10% TGFb**	**KSFM CTL**	**KSFM TGFb**
Mean	0,9844	1,596	1,015	1,465	0,9782	1,769	1,000	1,962
Std. Deviation	0,08862	0,2264	0,09755	0,09860	0,1605	0,3270	0,04548	0,2608
Significance (vs CTL)		****		****		****		****
EGR1 expression (n=6-12/group)								
	DMEM 5% CTL	**DMEM 5% TGFb**	**DMEM 10% CTL**	**DMEM 10% TGFb**	**F12 10% CTL**	**F12 10% TGFb**	**KSFM CTL**	**KSFM TGFb**
Mean	1,000	1,543	1,000	0,7109	1,000	1,913	1,000	0,7173
Std. Deviation	0,07682	0,4133	0,1066	0,1822	0,08827	0,4095	0,07953	0,2557
Significance (vs CTL)		***				****		

*Means ± SD (n=6–12/group), normalized to GAPDH, relative to controls. *** $p < 0.001$ vs. control (Mann-Whitney U test) (63).*

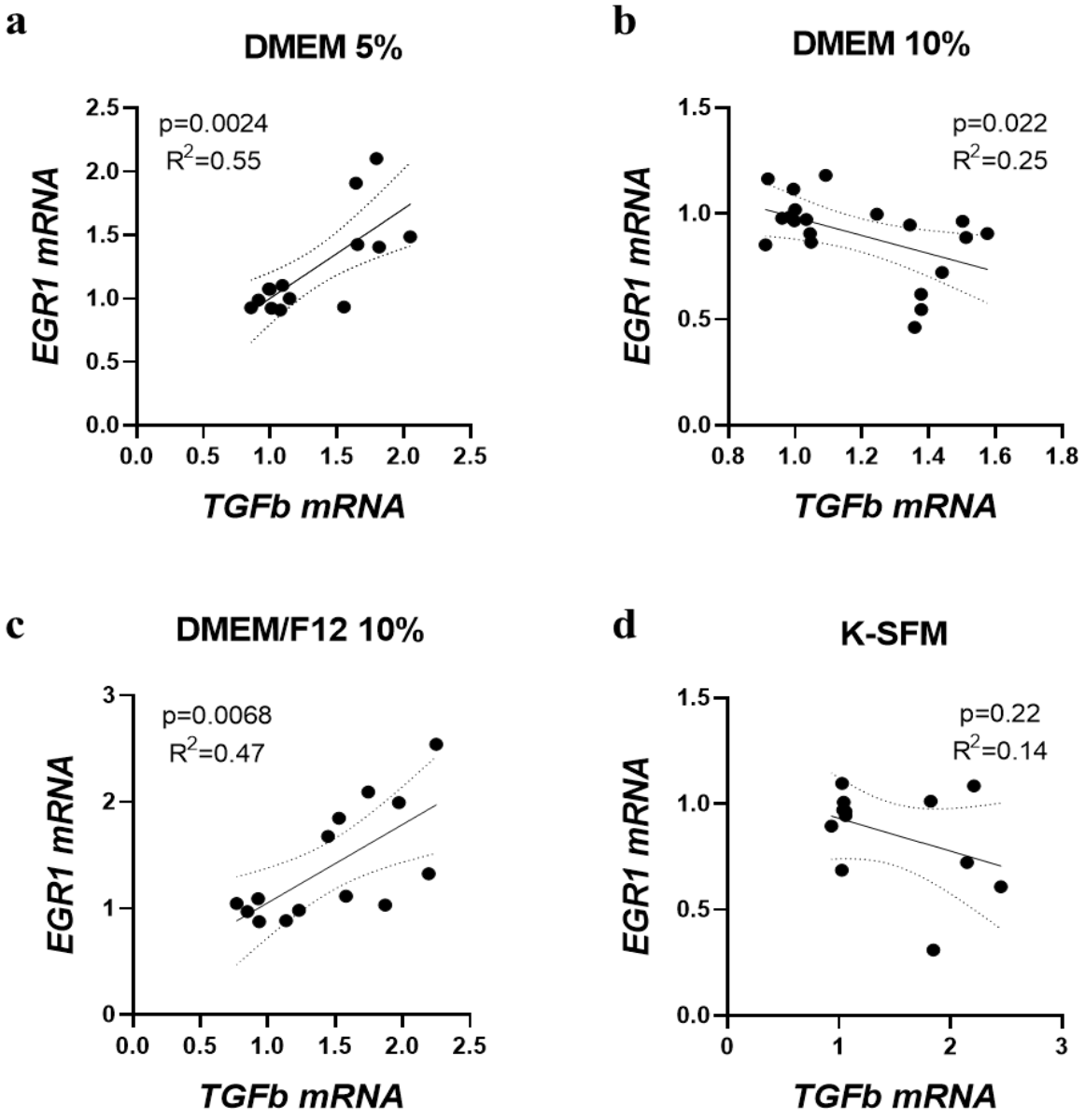

Figure 1. Pearson correlation analysis of *EGR1* mRNA expression in HK-2 samples cultured in different cell culture medium after 24 h TGF-β1 stimulation. *(a) DMEM 5% FBS, (b) DMEM 10% FBS (c) DMEM/F12 10% FBS, (d) KSFM (63).*

Evaluation of additional fibrosis- and inflammation-related markers revealed that *COL1A1* was robustly induced in every medium. Importantly, both *TIMP1* and *LGALS3* mRNA displayed statistically significant upregulation exclusively in DMEM 5% FBS after TGF-β1 treatment (Fig. 2).

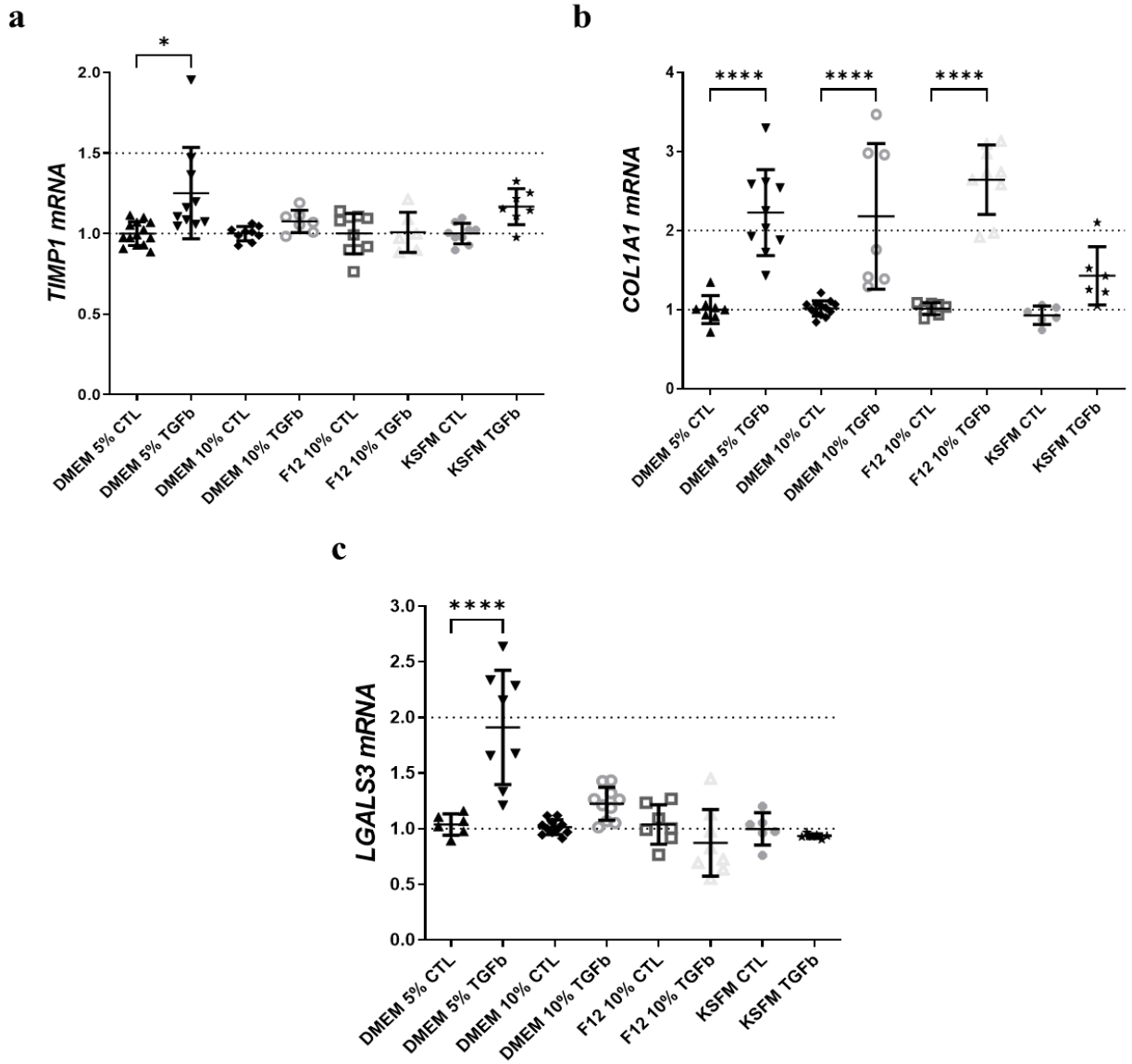

Figure 2. Relative mRNA expression of (a) *TIMP1*, (b) *COL1A1*, and (c) *LGALS3* in HK-2 cells after TGF-β1 stimulation in the four media formulations. Individual data points and mean ± SD are shown (n = 6–12). TIMP1 and LGALS3 were significantly upregulated only in DMEM 5% FBS, whereas COL1A1 was strongly induced in all conditions. *p ≤ 0.05, **p ≤ 0.01 and ***p ≤ 0.001 Kruskal-Wallis test (63).

Based on the most consistent TGF-β1-induced EMT signature, the strongest correlation between key early response genes, and the selective induction of *TIMP1* and *LGALS3* (both of which are

highly associated with fibrogenesis and NSAID-associated inflammatory pathways), DMEM supplemented with 5% FBS was chosen as the optimal culture condition for all subsequent experiments investigating NSAID-induced renal tubular injury and fibrosis.

4.1.2 NSAID administration causes dose-dependent cytotoxicity in vitro

A dose-dependent increase in NSAID cytotoxicity in HK-2 (Fig. 3) cells is observed, with IND being the least toxic amongst the NSAIDs considered. Celecoxib (CEL) showed minimal toxicity at lower concentrations (CEL0.72 and CEL2.1) but induced substantial cytotoxicity at higher concentrations (CEL4.3 and CEL8.7). Naproxen (NAP) exhibited a pronounced increase in toxicity, with the most significant effect observed at NAP110.

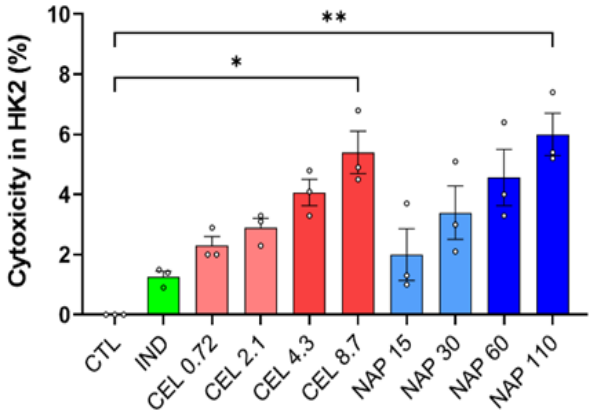

Figure 3. Dose-dependent toxicity of NSAIDs on renal epithelial cells in vitro. The cytotoxicity of celecoxib (CEL) and naproxen (NAP) on HK-2 cells exhibited a dose-dependent increase, with significant toxicity observed only at the highest doses. These findings informed the selection of NSAID concentrations for subsequent cellular experiments (n=3/group, Kruskal-Wallis test with Dunn's post hoc test; *p<0.05, **p<0.01) (64).

4.1.3 Induction of fibrosis-related pathways and autophagy dysregulation in HK-2 and IMCD cells following treatment with high-dose of NSAIDs

Exposure of HK-2 cells to NSAIDs triggered a marked dose-dependent increase in the expression of genes related to fibrosis and autophagy. Key fibrotic markers—such as *TGFB1*, *ACTA2* (α-SMA), *TIMP1*, *MMP9*, *COL1A1*, and *LCN2* (Fig. 4a-f) — showed elevated transcript levels. Similarly, genes encoding the Activator protein-1 (AP-1) transcription factor components *JUN* and *FOS*,

along with the transcription factors *EGR2* and *EGR1*, were significantly upregulated (Fig. 5a-d). The most prominent effects were observed at the highest concentrations of celecoxib (CEL8.7) and naproxen (NAP110), whereas lower doses produced little to no change. In contrast, indomethacin did not substantially alter the expression of these genes. This pattern of upregulation was also confirmed in IMCD cells (64) , indicating a consistent response across different renal cell types.

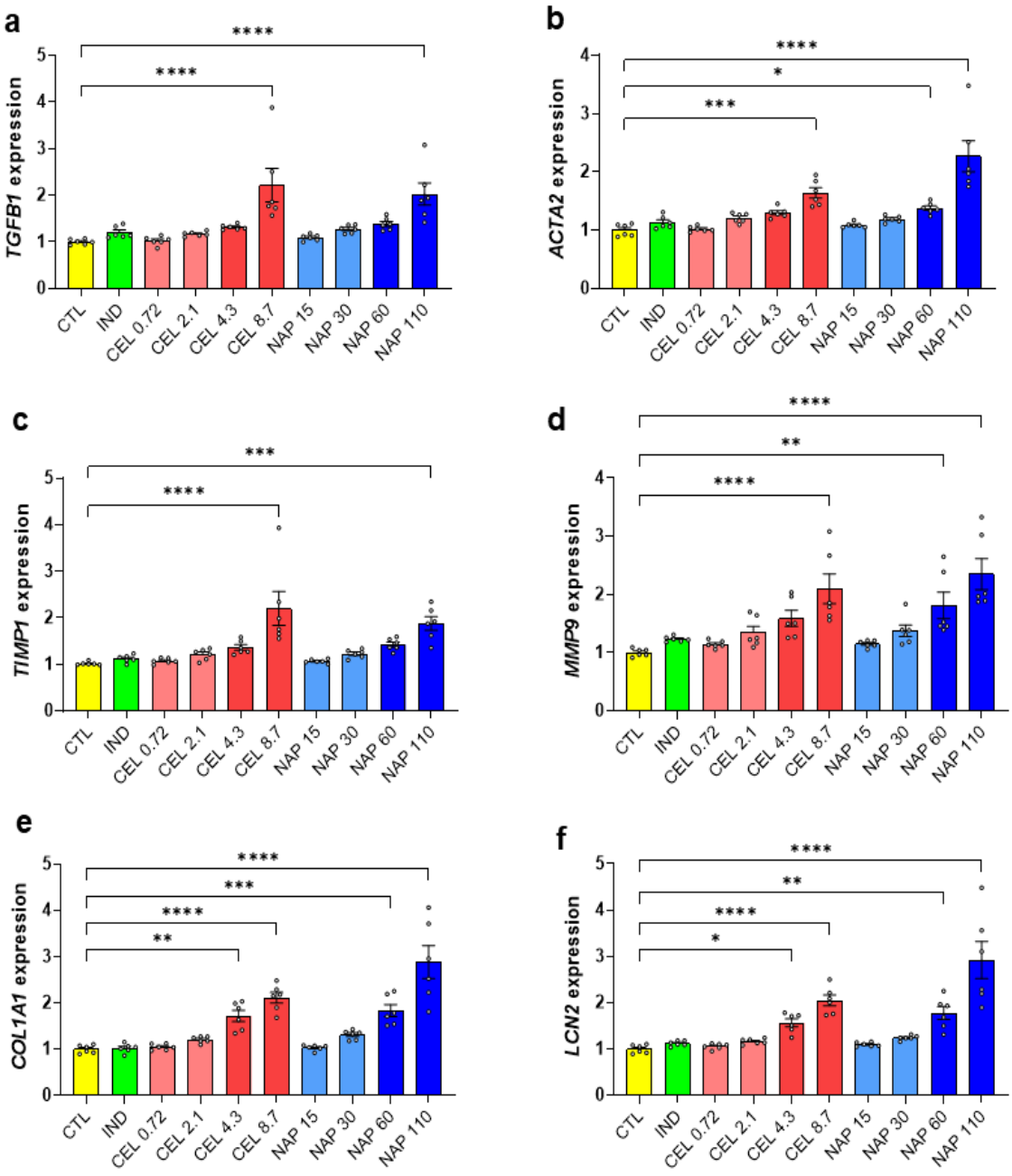

Figure 4. HK-2 cells treated with the highest concentrations of celecoxib (CEL8.7) and naproxen (NAP110) showed a meaningful increase in mRNA levels of profibrotic markers when compared to untreated cells. The markers are TGFB1 (a), α-SMA (ACTA2) (b), TIMP1 (c), MMP9 (d), COL1A1 (e), and LCN2 (f). Data are mean ± SD. Statistical comparisons were performed by one-way analysis of variance ANOVA and the Holm-Sidak test, *$p < 0.05$, **$p < 0.01$, ***$p < 0.001$, ****$p < 0.0001$ (64).

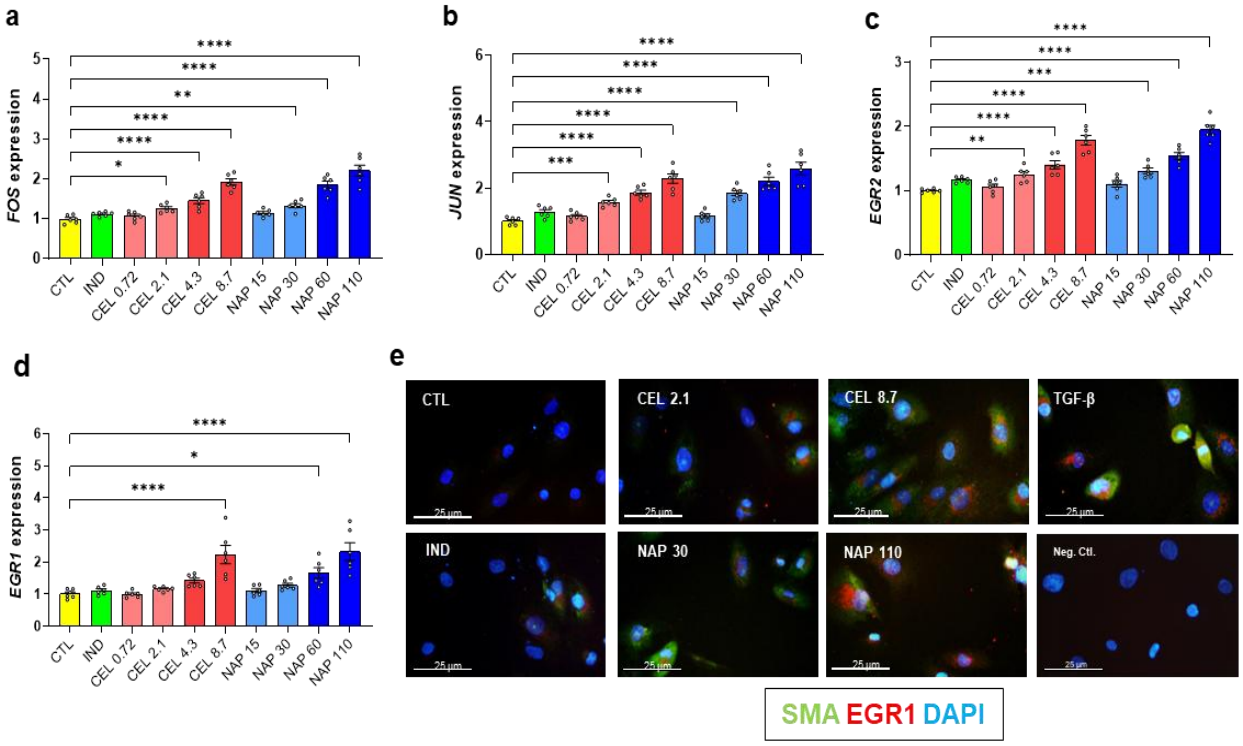

Figure 5. Induction of pro-fibrotic gene and protein expression in HK-2 cells by high-dose NSAIDs. Treatment with elevated concentrations of celecoxib and naproxen resulted in significantly increased mRNA expression of the transcription factors FOS (a) and JUN (b), EGR2 (c) and EGR1 (d). These transcriptional changes were consistent with observations at the protein level. Immunocytochemical analysis (e) confirmed that a 24-hour exposure to both low and high doses of celecoxib and naproxen enhanced the expression of EGR1 (red) and α-SMA (green) proteins. TGF-β was used as a positive control for the induction of both proteins (scale bar: 25 µm; nuclei counterstained with DAPI). Data indicate mean ± SD. One-way ANOVA followed by the Holm-Sidak post hoc test was used for statistical analysis (*$p < 0.05$, ** $p < 0.01$, ***$p < 0.001$, ****$p < 0.0001$) (64).

The mRNA levels of these autophagy mediators, *BECN1*, *ATG7*, *CLU* and *LC3A* (Fig 6a-d) were upregulated by treatment with the highest doses of celecoxib (CEL4.3, CEL8.7) and naproxen (NAP60, NAP110). The highest upregulation was clear with CEL8.7 and NAP110. The upregulated expression level of these autophagy markers was also confirmed in the IMCD cells (64) .

We analysed the protein levels of LC3 and SQSTM1 (p62) to assess the activity of autophagy. High-dose NSAIDs (CEL8.7, NAP110) increased the LC3-II to LC3-I ratio (Fig. 6e), further suggesting that the increase in LC3-II was due to increased autophagosome formation. Simultaneously, an increase in levels of SQSTM1/p62, a protein that is usually degraded in the course of autophagy flux (Fig. 6f), was also observed. The elevated LC3-II/I ratio combined with the accumulation of p62 in HK-2 cells exposed to these conditions may indicate an unsuccessful completion of autophagic flux.

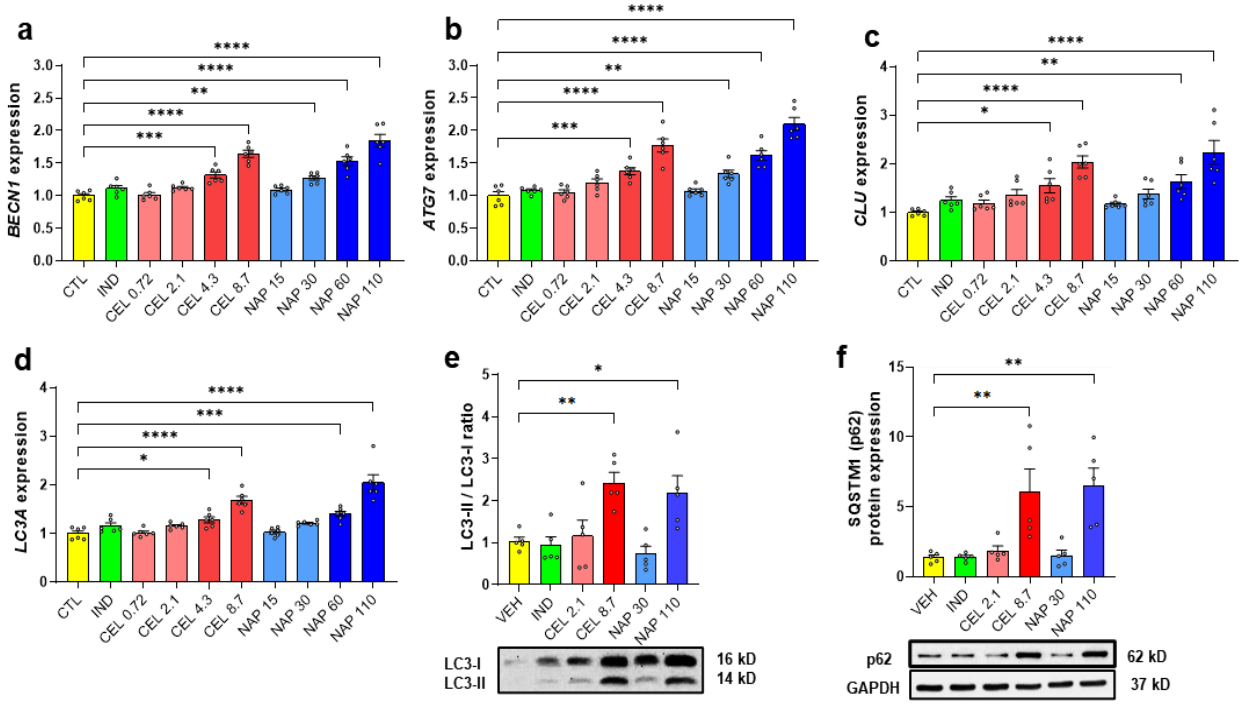

Figure 6. High-dose NSAIDs induce autophagy-related changes in HK-2 cells. The mRNA levels of autophagy markers BECN1 (a), ATG7 (b), CLU (c), and LC3A (d) were increased with higher doses of celecoxib (CEL4.3, CEL8.7) and naproxen (NAP60, NAP110) treatments. Results of immunoblotting showed that the LC3-II/LC3-I ratio (e) was considerably increased in a dose-dependent manner (CEL8.7, NAP110) due to an increase in the number of autophagosomes and p62 protein accumulation, resulting in defective autophagic degradation. All quantitative data were expressed as the mean ± SD. One-way analysis of variance or ANOVA assessed differences statistically, and then the Holm-Sidak post hoc test was used (*$p < 0.05$, **$p < 0.01$, ***$p < 0.001$, ****$p < 0.0001$) (64).

4.1.4 Induction of stress-response pathways by high-dose NSAIDs in cultured tubular epithelial cells

In HK-2 cells, exposure to the highest concentrations of CEL and NAP resulted in a marked upregulation of *HMOX1* mRNA levels (Fig. 7a). *HIF1A* gene expression was also significantly induced by CEL4.3, CEL8.7, NAP60, and NAP110 treatments, with the most substantial increases seen in the CEL8.7 and NAP110 groups (Fig. 7b). Consistent with the mRNA data, HMOX1 protein abundance was considerably higher in HK-2 cells treated with CEL8.7 and NAP110 (Fig. 7c). In parallel, both total AKT protein expression and its phosphorylation were selectively enhanced in the CEL8.7- and NAP110-treated cells (Fig. 7d). In contrast, CEL2.1 and NAP30 treatments produced no discernible effects on these parameters. In IMCD cells, the administration of high-dose CEL and NAP triggered a robust overexpression of both *Hmox1* and *Hif1a* transcripts (64).

4.1.5 Induction of renal tubular dilation and atrophy in rats after prolonged NSAID administration

Following the findings *in vitro*, we examined whether prolonged administration of CEL and NAP also damages the tubular structures. Kidney histology (Fig. 8) revealed statistically significant but mild structural alterations associated with high-dose NSAID administration. Compared to vehicle-treated controls (VEH), rats treated with CEL30 and NAP20 exhibited tubular dilatation and atrophy (b, c). The tubular luminization also increased, and the epithelial walls thinnered (a). Tubular cell density was decreased. Mononuclear cell infiltration (not significant) was slightly increased in the CEL30 and NAP20 groups (Fig. 8d).

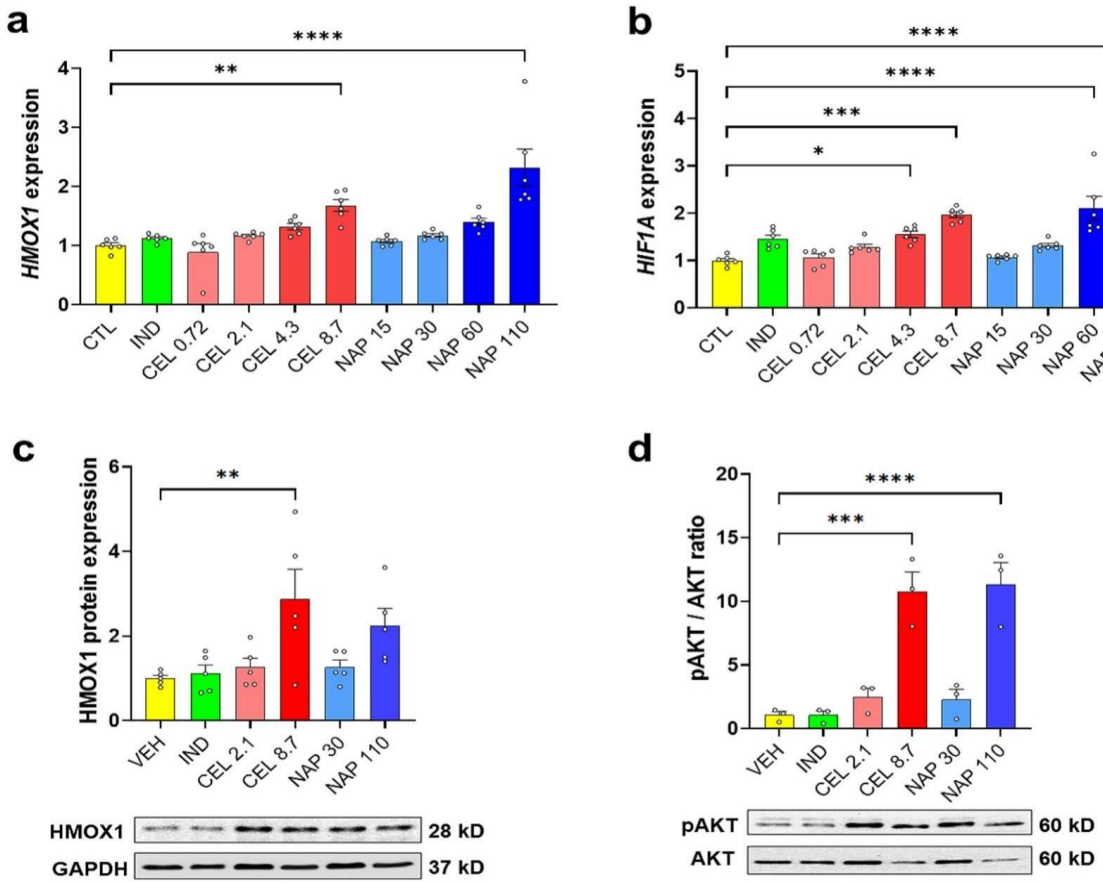

Figure 7. Activation of stress-signaling pathways in HK-2 cells following NSAID exposure.

The amount of the HMOX1 gene (a) and HIF1A mRNA (b) increased in the CEL8.7 and NAP110 groups, whereas HMOX1 protein levels (c) were markedly elevated only in the CEL8.7 group. The pAKT/AKT ratio (b) was increased in response to high-concentration CEL and NAP treatments. Indomethacin showed no notable effects. Data are expressed as mean ± SD and evaluated using one-way ANOVA with Holm–Sidak post hoc test; *p < 0.05, **p < 0.01, ***p < 0.001, ****p < 0.0001 (64).

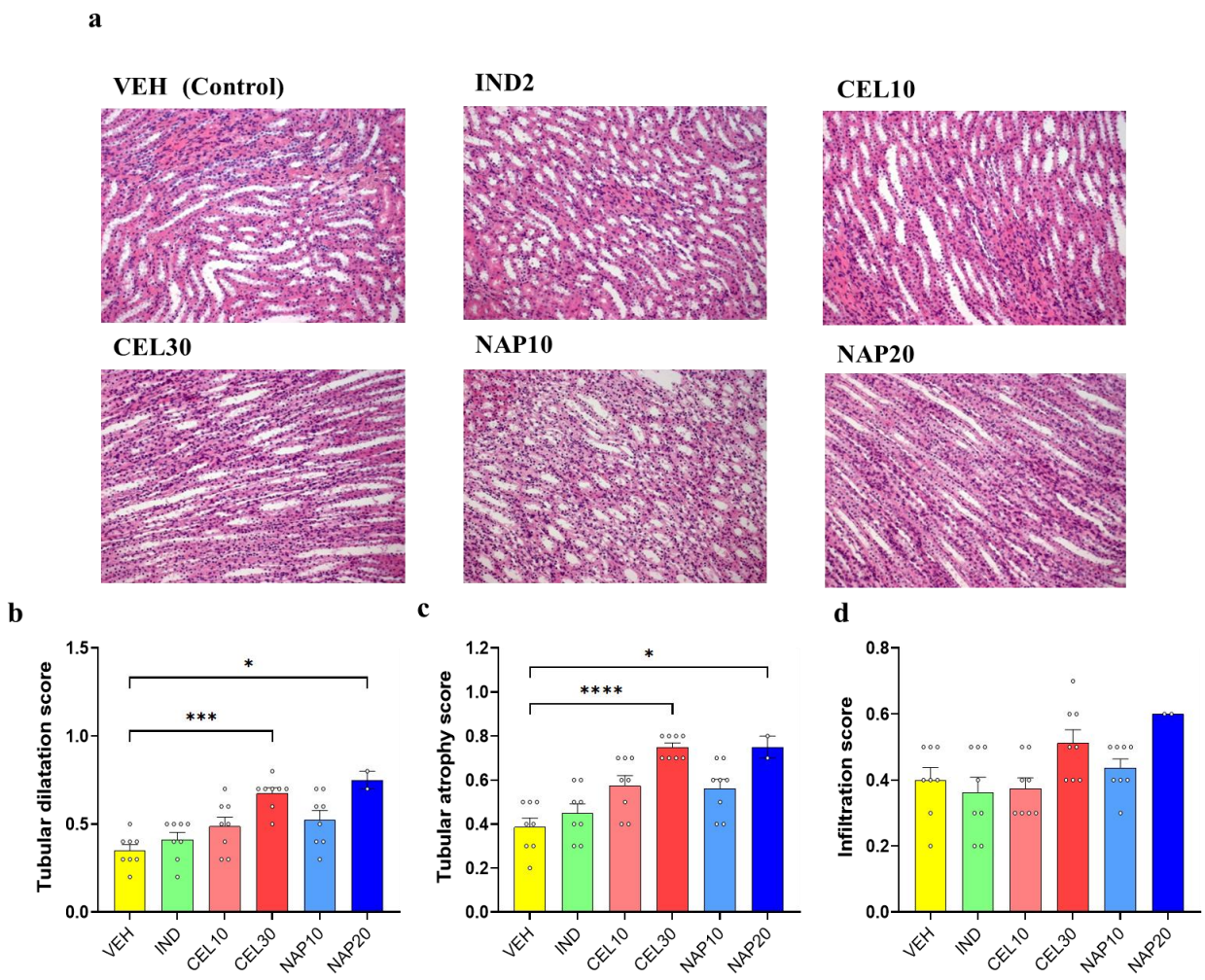

Figure 8. Mild renal structural modifications due to high-dose NSAID administration. Histological images of the kidney medulla (a; H&E staining, 200× magnification) demonstrate dose-dependent NSAID effects, with mild tubular dilatation (b) and atrophy (c) observed in the CEL30 and NAP20 groups. Mononuclear cell infiltration remained unaffected by the treatments (d). Data are expressed as mean ± SD and analysed using the Kruskal-Wallis test with Dunn's post hoc test; *$p < 0.05$, ***$p < 0.001$, ****$p < 0.0001$ (64).

4.1.6 Treatment with NSAIDs stimulated renal fibrotic pathways in a dose-dependent manner

High-dose NSAIDs triggered significant and dose-dependent activation of fibrosis-related pathways in the renal medulla (Fig. 9). Administration of celecoxib (CEL30) and naproxen (NAP20) strongly induced mRNA expression of *Tgfb1*, *Timp1*, *Col1a1* (Fig. 9a, b, e), *Egr1* (Fig.

10a), and the distal tubular injury marker *Lcn2* (Fig. 9f). In addition, expression of the AP-1 components *cFos* and *cJun* was markedly upregulated (Fig. 9c, d). The number of EGR1-positive cells was also substantially higher (Fig. 10b, c), with naproxen producing a stronger response than celecoxib. Notably, even low-dose naproxen (NAP10) significantly elevated the expression of all these mediators. These observations align closely with our earlier *in vitro* findings in HK-2 and IMCD cells.

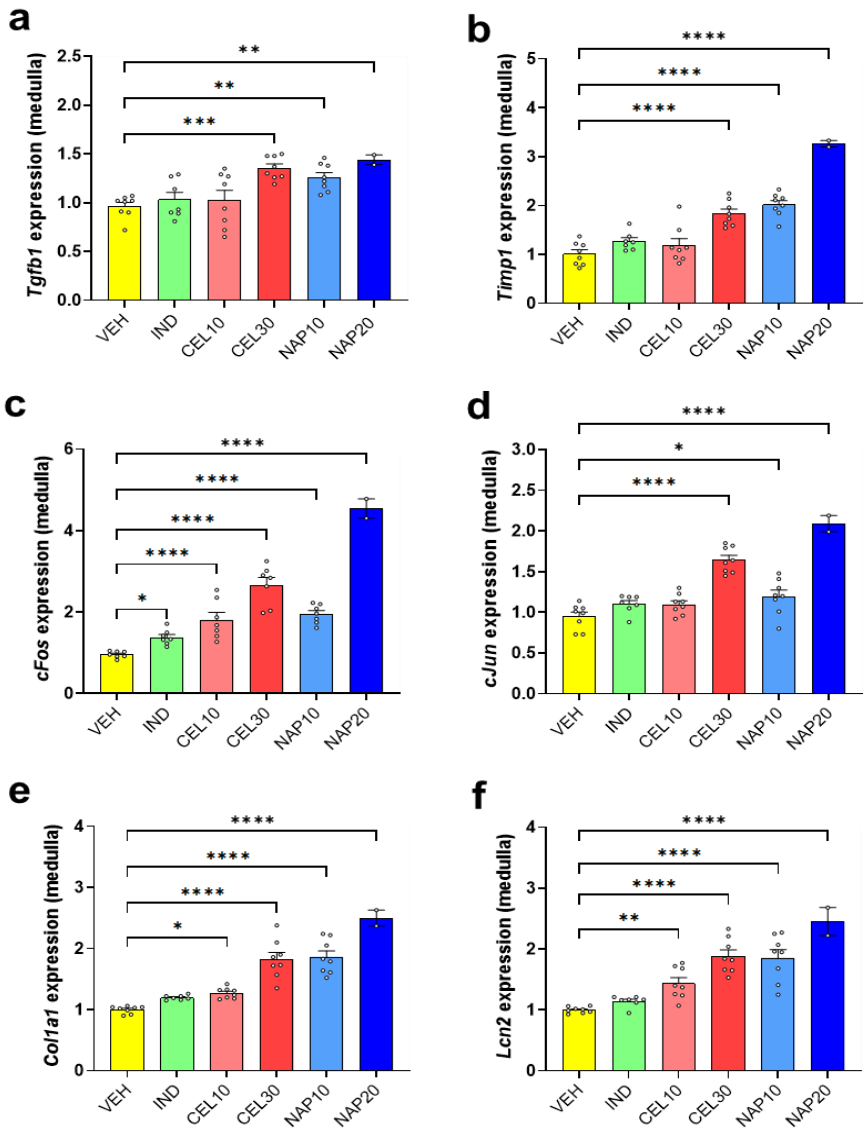

Figure 9. Dose-dependent alterations in renal medullary gene expression following NSAID treatment. Molecular analysis revealed a significant upregulation of several key genes in the kidney medulla of treated animals. Higher doses of celecoxib (CEL30) and low and high doses of

naproxen (NAP10, NAP20) marked mRNA upregulation of the profibrotic mediators Tgfb1 (a), Timp1 (b), and Col1a1 (e), the AP-1 transcription factor components cFos (c) and cJun (d), and the tubular cell injury marker Lcn2/NGAL (f). Mean ± SD. Number for each treatment group, except for NAP20 (n=2 due to morbidity earlier in the experiment) was 8. Statistical analysis was performed using one-way ANOVA and the Holm-Sidak post hoc test (*p < 0.05, ***p < 0.001, ****p < 0.0001) (64).

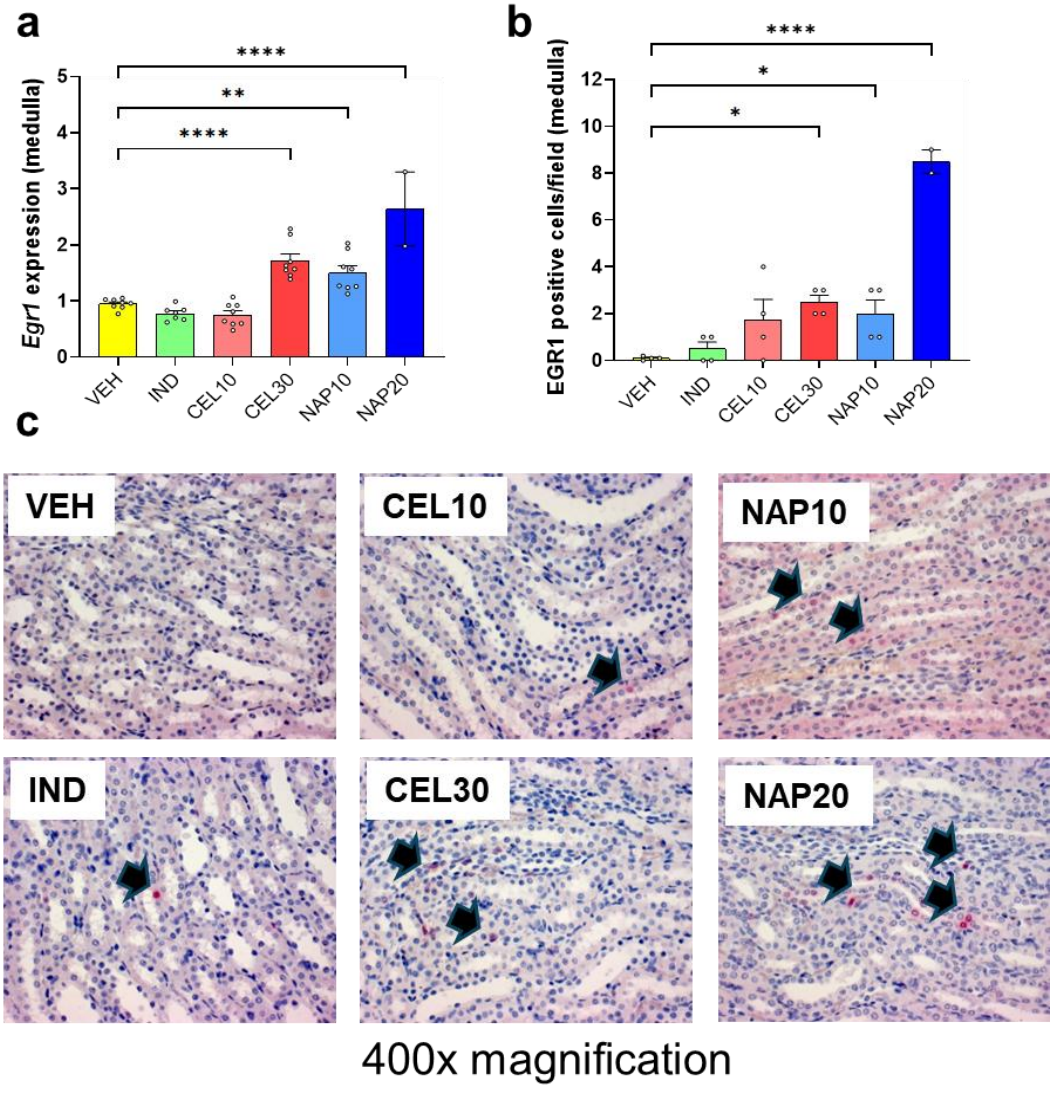

Figure 10. Medullary EGR1 expression is upregulated by NSAID treatment. Medullary expression of Egr1, a stress-response transcription factor, was upregulated by treatment with high-dose celecoxib (CEL30) and low- and high-dose naproxen (NAP10 and NAP20) (a). This

transcriptional increase was confirmed at the protein level by immunohistochemistry, which revealed a substantial rise in the number of EGR1-positive cells within the medulla (b, c). Representative images are shown at 400× magnification, with quantitative analysis performed in a blinded manner. Data are expressed as mean ± SD, with group sizes of n=8 for all treatments except NAP20 (n=2). Statistical significance was determined using one-way ANOVA followed by the Holm–Sidak post hoc test (*$p < 0.05$, ***$p < 0.001$, ****$p < 0.0001$) (64).

4.1.7 Autophagy impairment and oxidative stress are induced in the renal medulla by high-dose NSAIDs.

High-dose NSAIDs markedly altered autophagy markers in the renal medulla, with significant upregulation of mRNA expression of the autophagy genes *Atg7* (Fig. 11a) and *Becn1* (Fig. 11b) in animals treated with high-dose celecoxib (CEL30) and naproxen (NAP20) compared with vehicle controls. Western blot analysis revealed a substantial increase in the LC3-II/LC3-I ratio (Fig. 11c), consistent with enhanced autophagosome formation. However, this was accompanied by a pronounced accumulation of SQSTM1/p62 protein (Fig. 11d) and persistently elevated LC3-II levels, indicating impaired autophagic flux despite increased autophagosome generation. These findings demonstrate that high-dose celecoxib and naproxen disrupt the completion of autophagy, leading to blocked autophagic degradation in the renal medulla (64, 66)

In the renal medulla, NAP20 and CEL30 induced a strong upregulation in the expression of *Hmox1* (Figure 12a) and *Hif1a* (Figure 12b) mRNA; the highest level of these genes was observed in the naproxen-treated groups. Thereby, in the medulla, the exposure to high-dose NSAIDs increased the level of HMOX1 (Fig. 12c) and the phosphorylation of AKT (Fig. 12d). Collectively, these results show the *in vivo*, dose-dependent activation of hypoxia-response and oxidative-stress and survival pathways, which are consistent with the same trends observed for HK-2 and IMCD cells.

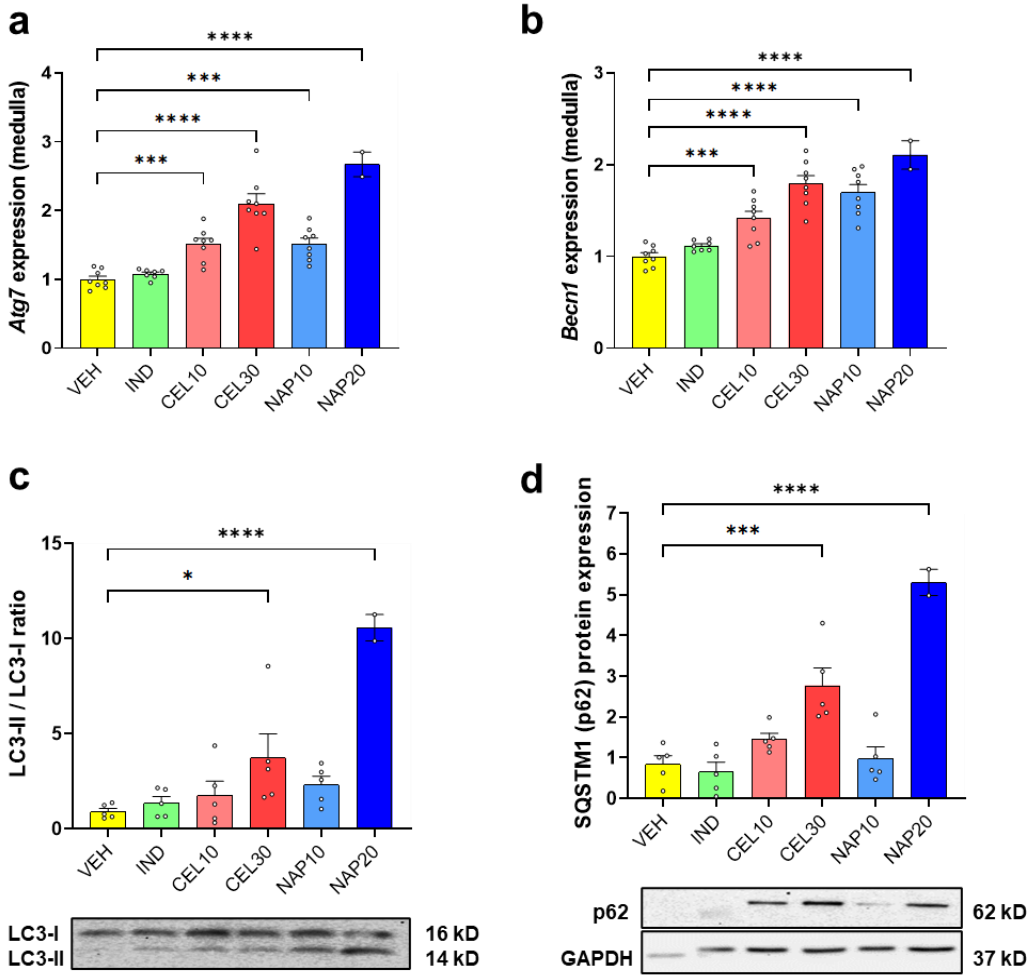

Figure 11. Dysregulation of autophagy in the renal medulla by high-dose NSAIDs. *Treatment* with high-dose oral celecoxib (CEL30) and naproxen (NAP20) (high dose) caused a marked increase in the mRNA expression of the autophagy genes Atg7 and Becn1 (a, b) and an increase in the ratio of LC3-II/LC3-I (c), indicating that both drugs considerably increased autophagosome formation in medullary tissue. At the same time, SQSTM1/p62 protein accumulation (d) was increased, indicating a blockage of late stages of autophagic degradation. Data are shown as mean

± SD. Statistical comparisons were made using one-way ANOVA, then the Holm-Sidak post hoc test (*p < 0.05, ***p < 0.001, ****p < 0.0001) (64).

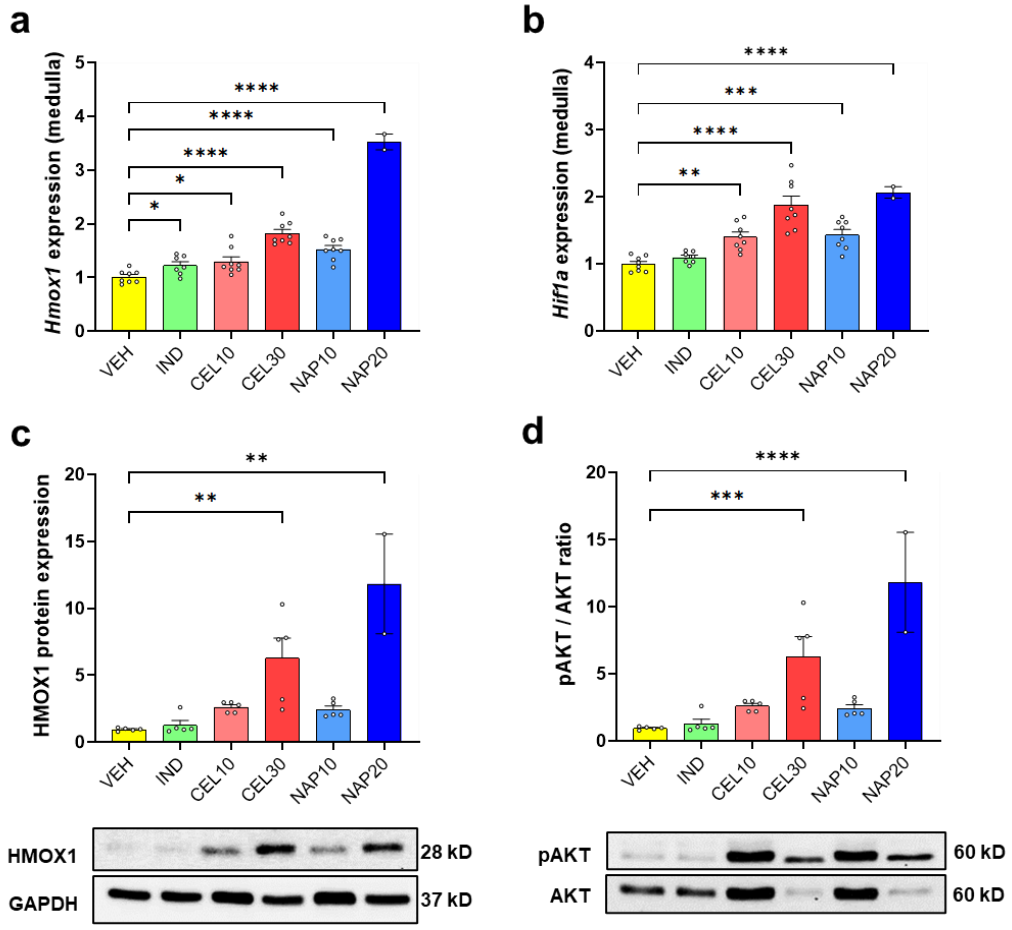

Figure 12. NSAID-mediated regulation of oxidative stress in the renal medulla. Hif1a and Hmox1 (a, b) mRNA levels were significantly increased across all NSAID treatments, with the highest induction seen in the NAP20 and CEL30 groups. HMOX1 (c) protein abundance was markedly elevated in animals receiving high-dose NSAIDs. The pAKT/AKT ratio (d) was significantly higher in the high-dose groups, indicating activation of survival signaling. Data are presented as mean ± SD. Statistical comparisons were performed by one-way ANOVA and the Holm–Sidak post hoc test (*p < 0.05, ***p < 0.001, ****p < 0.0001).

4.2 NSAID-Induced Enteropathy

4.2.1 Indomethacin-induced changes in intestinal antimicrobial peptides and hematology parameters

Acute indomethacin (IND, 20 mg/kg) administration caused time-dependent upregulation of small intestinal cathelicidin (Camp) mRNA expression from 12 hours post-treatment onward, while α-defensin 5 (Defa5) and β-defensin 2 (Defb2) showed high variability without significant overall changes (Fig. 13a-b). Cathelicidin expression correlated positively with inflammatory genes including IL1B and TNF, whereas defensins had weaker associations (Fig. 13d). Chronic IND treatment (2 mg/kg twice daily for 14 days or 4 mg/kg twice daily for 6 days) similarly upregulated cathelicidin, with additional increase in α-defensin 5 in the higher dose group and variable β-defensin 2 expression (Fig. 14 a-c). Hematology parameters in the acute model revealed reductions in red blood cell indices and increases in platelet parameters at multiple time points (Table 3).

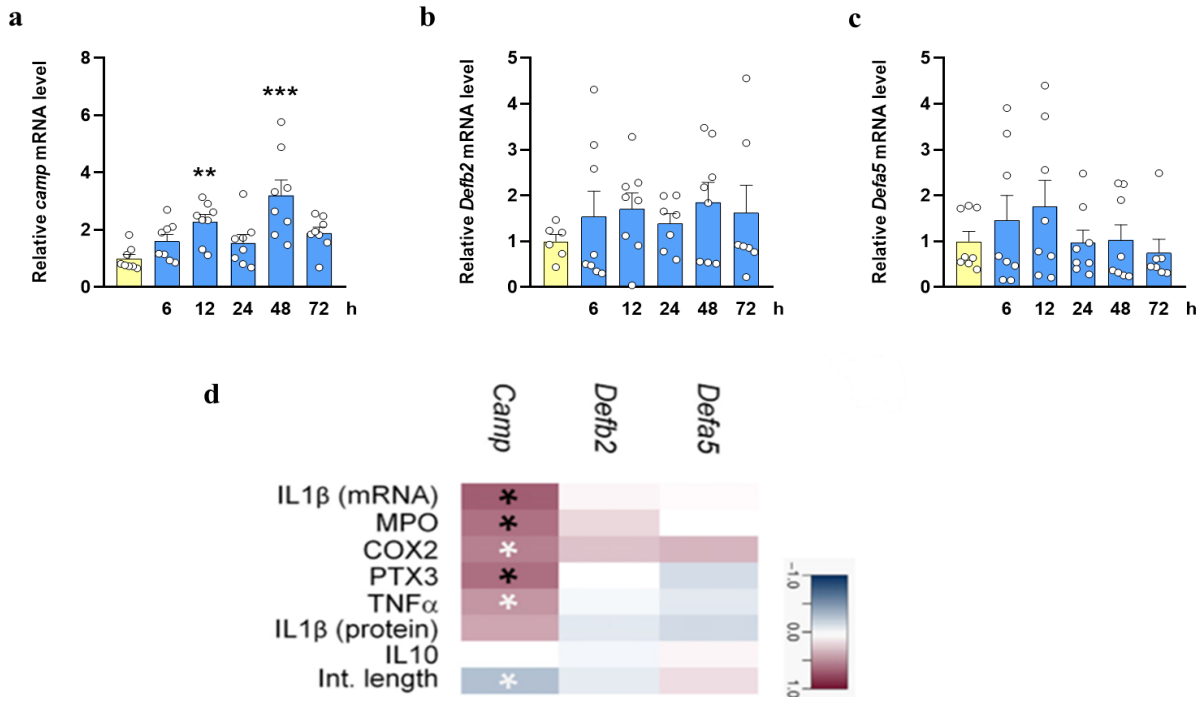

Figure 13. Acute indomethacin administration modulates antimicrobial peptide expression and its correlation with inflammation in the rat small intestine. The mRNA levels of (a) Cathelicidin (Camp), (b) β-defensin 2 (Defb2), and (c) α-defensin 5 (Defa5) were measured over a 72-hour period following a single administration of indomethacin at 20 mg/kg. Cathelicidin showed significant upregulation at 12 h and 48 h, whereas β-defensin 2 and α-defensin 5 exhibited

high variability without significant changes. One-way ANOVA followed by Holm–Sidak post hoc test. n = 5–8/group. *p < 0.05, **p < 0.01, ***p < 0.001. (d) Heatmap of Spearman's correlation coefficients between the three AMPs and inflammatory markers (IL-1β mRNA and protein, MPO, COX2, PTX3, TNFα, IL-10, intestinal length). Significant correlations (Benjamini–Hochberg false discovery rate correction) are denoted by asterisks (55).

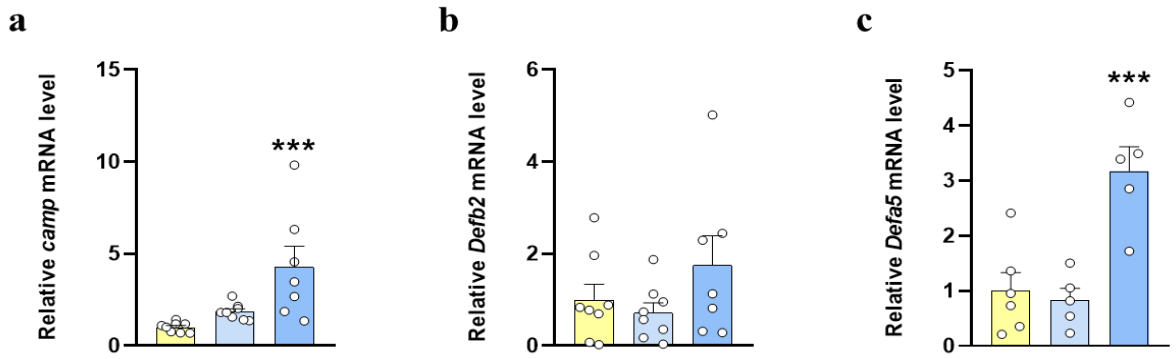

Figure 14. Effects of chronic indomethacin administration on small intestinal antimicrobial peptide mRNA expression in rats. (a) Cathelicidin (Camp), (b) β-defensin 2 (Defb2), and (c) α-defensin 5 (Defa5) expression after repeated dosing with 2 mg/kg IND twice daily for 14 days or 4 mg/kg IND twice daily for 6 days. Both Cathelicidin and α-defensin 5 showed significant upregulation exclusively in the higher-dose (4 mg/kg) group, whereas β-defensin 2 remained variable without consistent change. Statistical significance was determined using one-way analysis of variance (ANOVA) with Holm–Sidak post hoc test. Group sizes ranged from 5 to 8 animals. Significance levels are denoted as follows: *p < 0.05, **p < 0.01, and ***p < 0.001 (55).

Table 3. Hematological parameters in rats exposed to long-term indomethacin treatment.

Hematological parameters	Unit	VEH		IND 2		IND 4	
		Mean	***SEM***	***Mean***	***SEM***	***Mean***	***SEM***
RBC	(10^12/L)	8.1	0.2	7.4	0.2	**3.8*****	0.3
HGB	(g/dL)	15.3	0.3	**13.9***	0.2	**6.9*****	0.5
HCT	(%)	45.9	0.8	**42*****	0.7	**22.2*****	1.1
MCV	(fL)	56.8	0.4	56.6	0.5	58.9	1.5
MCH	(pg)	19.0	0.2	18.7	0.2	18.2	0.3
MCHC	(g/dL)	33.3	0.2	33.1	0.3	**30.9*****	0.9
CHCM	(g/dL)	31.6	0.1	31.4	0.3	**30.1*****	0.7
CH	(pg)	17.9	0.2	17.7	0.2	17.6	0.3
RDW	(%)	11.2	0.5	11.5	0.4	**14.7*****	1.1
HDW	(g/L)	2.4	0.1	2.4	0.1	**3.4*****	0.1
PLT	(10^9/L)	760.3	37.8	944.4	62.1	**1658.2*****	173.5
MPV	(fL)	7.1	0.2	7.3	0.2	**11.6*****	0.5
PCT	(%)	0.5	0.03	0.7	0.05	**1.9*****	0.1
PDW	(%)	60.4	1.7	60.8	1.7	112.1	2.5
WBC	(10^9/L)	8.2	0.2	9.8	1.02	7.2	1.2
NEUT	(%)	11.4	1.1	**24.05*****	3.3	**27.6*****	3.3
LYMPH	(%)	84.5	1.2	**72.1*****	3.4	**63.5*****	4.8
MONO	(%)	2.0	0.2	1.9	0.3	**3.3***	0.8
EOS	(%)	1.0	0.1	1.1	0.1	**0.4***	0.1
BASO	(%)	0.1	5. 7	0.1	0.02	0.1	6.2
LUC	(%)	1.0	0.1	0.8	0.1	**5.2*****	0.9
MPXI	(10^9/L)	-1.8	0.5	-3.8	0.7	**-11.1**	4
RETIC	(%)	2.26	0.106	3.1	0.51	**13.98****	3.29

*Data are expressed as mean ± standard error of the mean (SEM) with eight animals per group. Statistical significance was assessed using one-way ANOVA followed by Holm–Sidak post hoc test; *p < 0.05, **p < 0.01, and ***p < 0.001 compared with the vehicle-treated group (55).*

5 DISCUSSION

5.1 NSAID-Induced Renal Damage

Our first study demonstrated that nonsteroidal anti-inflammatory drugs (NSAIDs), whether selective or nonselective COX inhibitors, exhibit dose-dependent effects on autophagy, fibrosis, and stress responses in HK-2 and IMCD cells in vitro, as well as in rat kidneys in vivo. High-dose celecoxib or naproxen induced the transcription factors EGR1, AP-1, and impaired autophagy, as evidenced by the accumulation of p62, and an increase in the LC3-II/I ratio. These modifications result in the accumulation of impaired cellular components, including misfolded proteins and malfunctioning mitochondria (38). Moreover, compensatory reactions, such as elevated hemoxygenase-1 levels and AKT phosphorylation, indicate the cells' efforts to mitigate the stress caused by the drugs at elevated doses. The findings underscore the critical need for accurate NSAID dosing to avoid kidney damage and promote the advancement of innovative therapeutic approaches to reduce drug toxicity.

Continued administration of higher doses of celecoxib (30 mg/kg) and naproxen (20 mg/kg) induced the expression of several fibrosis markers (*Tgfb1*, *Timp1*, *Egr1*), as well as AP-1 components (*Fos* and *Jun*), in the kidney medulla. The medulla have distinct vascular and metabolic features, consisting of reduced oxygen tension and elevated metabolic demands, making it susceptible to enhanced oxidative stress and drug-induced injury (67). The higher expression of renal medullary *Lcn2* (NGAL) confirms this claim. Previous in vitro and in vivo studies have also shown that injury to the renal medulla induces immediate elevation of both TGF-β and EGR1 (68). Furthermore, in our current investigation, naproxen demonstrated a more pronounced effect on the expression of these markers compared to celecoxib, aligning with prior findings that indicated a more significant decline in GFR associated with naproxen, potentially due to its more potent inhibition of COX-1 and COX-2 relative to celecoxib (69). The non-selective COX inhibitor IND at the dose utilized did not have effects like celecoxib or naproxen. Based on prior studies, we chose a daily IND dose that completely inhibits COX without severe nephrotoxicity. Chronic oral treatment with 10 mg/kg/day resulted in papillary necrosis in 25% of rats, which is twofold higher than in our study (4 mg/kg/day; human equivalent dose: 39 mg/day) (70). Our investigation found that only CEL and NAP increased tubular damage marker NGAL (Lcn2) expression. Our investigation found that only CEL and NAP increased tubular damage marker NGAL (Lcn2) expression, even at human-equivalent doses (HEqDs) within recommended ranges (65). Our

research demonstrates that the renal effects of CEL and NAP do not depend upon COX-inhibition (71), highlighting the drug-specific and mechanistic differences in NSAID-induced renal effects. These NSAIDs may have different mechanisms, according to clinical evidence. Naproxen and celecoxib dose decrease is recommended for CKD patients, but not that of indomethacin (65). Children who had heart surgery showed subclinical kidney impairment with large urine NGAL increases within 72 h after receiving NSAIDs, suggesting a risk for renal adverse events even in healthy kidneys (72). The prior clinical trial found that celecoxib had fewer adverse renal events than naproxen despite chronic treatment (73), while our rat investigation found no differences in renal medullary effects.

In HK-2 and IMCD cells exposed to high doses of celecoxib (8.7 μM) and naproxen (110 μM), the expression of several of the pro-fibrotic genes was upregulated, including *TGFB1*, *ACTA2* (α-SMA), *TIMP1*, *EGR1*, *EGR2*, as well as the AP-1 components *FOS, and JUN*. These results are consistent with some of the animal model studies. To ensure reliable and consistent modeling of TGF-β1-driven epithelial-mesenchymal transition (EMT) and fibrogenic responses in HK-2 cells, DMEM supplemented with 5% FBS was selected as the optimal culture medium, as it demonstrated the strongest TGF-β1-induced EMT signature, the highest correlation between *TGFB1* and *EGR1* expression (63). These results suggest that high-dose NSAIDs activate injury-associated signaling pathways (including TGF-β signaling) in HK-2 and IMCD cells. Increased *ACTA2* (α-SMA) expression indicates myofibroblast differentiation and epithelial-to-mesenchymal transition (EMT), which further supports the activation of TGF-β signaling. During EMT, mature myofibroblasts that are positive for α-SMA exhibit a contractile phenotype with characteristic stress fibers, produce extracellular matrix components, and contribute to tissue remodeling (74). This has been supported by the upregulation of transcription factors EGR1 and EGR2. EGR1 is an immediate early response gene that is rapidly upregulated by TGF-β and plays a role in collagen production. EGR2 is an EGR1 homolog that enhances fibrotic responses and is crucial for various processes; however, its role in kidney fibrosis was recently discovered (75). EGR2 is also transiently upregulated downstream of TGF-β signaling by the early response gene EGR1, which itself can upregulate collagen genes (76). EGR2 overexpression has been shown to increase in vitro and in vivo TGF-β1-induced fibrosis, while EGR2 knockdown decreases it (75). EGR1 has been identified in our own and other studies as an activator of collagen transcription and possibly as an autophagy modulator in pulmonary fibrosis (77, 78), both of which may contribute to fibrotic

progression. It still needs to be determined whether EGR1 has a potential role in modulating autophagy in kidney fibrosis. Furthermore, the AP-1 transcription factor complex has been activated by celecoxib and naproxen, and may provide a further mechanism for these drugs' pro-fibrotic effect. For instance, the expression of AP-1 protein components, including FOS and JUN, was reported to mediate renal medullary injury in rats subjected to chronic hyperosmolarity (77) and TGF-β-dependent kidney fibrosis in mice (75). Although COX-2 inhibition with dehydration has been shown to stimulate NF-κB activation and apoptosis in the renal medulla (79), the effects of these NSAIDs on renal AP-1 have not been previously examined. These effects are unlikely to be mediated by inhibition of COX activity, since celecoxib modulates AP-1 activity in the skin and brain (80, 81). These findings suggest an involvement of TGF-β signaling, the transcription factors EGR1 and EGR2, and AP-1 in NSAID nephrotoxicity and the potential for fibrogenesis in otherwise normal kidneys. It is likely that the activation of these pro-fibrotic pathways may also exacerbate pre-existing disease processes in which EGR1 or AP-1 are activated, such as diabetic nephropathy (82, 83).

Treatment with high-dose celecoxib and naproxen considerably increased the expression of markers of autophagy, *ATG7*, *BECN1*, and *LC3A*, in HK-2 cells and in kidney tissue, alongside increased LC3-II/I and p62 accumulation (84). The findings were consistent with other evidence that impairment of autophagy limits the clearance of damaged proteins and organelles, leading to impaired mitochondrial function, increased oxidative stress, which in turn exacerbated chronic cellular stress that drives the progression of kidney injury (85) . Although we cannot exclude the possibility that the deficiency of autophagy in tubular cells is due to injury, in the absence of direct evidence of cell damage on histological slides, an increasingly impaired autophagic flux likely plays a role in NSAID-associated tubular injuries; the defective autophagic degradation and consequent intracellular accumulation of p62 can lead to the activation of inflammatory mediators such as NF-κB and, consequently, tissue damage (86).

Autophagy has also been reported to play a protective role in renal fibrosis, and it has been shown that Beclin-1 and LC3 inhibit collagen deposition and regulate the TGF-β1 signaling pathway. Deficiencies of these proteins in animal models shown an increase in the degree of fibrosis (87, 88), thus reinforcing the protective role of autophagy on oxidative stress and fibrosis. Impaired renal autophagic activity, as indicated by SQSTM1/p62 accumulation, was reported in kidneys from diabetic mice and rats (89, 90) and in tubular cells isolated from kidney biopsies of patients

with type 2 diabetes (91). These observations raise the possibility that restoring autophagic flux may represent a new therapeutic strategy targeting renal injury and progression of NSAID-associated nephropathy.

Increased HMOX1 expression and pAKT phosphorylation in HK-2 cells and mouse kidneys induced by higher doses of celecoxib and naproxen may compensate for oxidative stress caused by NSAIDs (92). The activation of HIF1 has been linked to increased expression of HIF1α (93) in both high-dose CEL and NAP treatments in vitro and in vivo. HMOX1 is part of the antioxidant system and can degrade heme into biliverdin, carbon monoxide, and free iron, thereby reducing oxidative stress (92). These data also agree with the report on celecoxib-treated glomerular mesangial cells, where oxidative stress induced HMOX1 gene expression through the JNK and PI3K signaling pathways (94). Although HMOX1 is protective in stress, the persistence of increased ROS levels may emphasize the possibility of oxidative damage. It could be a reason for caution in NSAID usage, particularly beyond therapeutic doses or in sensitive populations (95). Additional studies are needed to determine whether HMOX1 is solely an antioxidant enzyme or if it can also function as a damaging enzyme under certain conditions, particularly in the case of NSAID-induced renal cytotoxicity.

The strong activation of the AKT pathway highlights its crucial role in mediating cell survival and repair under conditions of cellular stress. The rapid activation of the PI3K/Akt pathway that we observed in all our experiments, and which has also been observed by others, likely represents an adaptive response to NSAID-induced oxidative stress. In particular, celecoxib-induced increases in phospho-AKT, as indicated by increased phosphorylated AKT, are protective against stress and enable the maintenance of homeostasis in response to an oxidative challenge (96). Both HMOX1 upregulation and AKT phosphorylation serve as stress responses against oxidative stress, while ROS regulates them to play a pathophysiological role in NSAID-induced nephrotoxicity. This provides some caution in the use of NSAIDs, especially at high doses, in vulnerable individuals. Further elucidation of the long-term effects of sustained upregulation of HMOX1 and pAKT/AKT signaling on NSAID-induced toxicity is warranted.

Our findings suggest that impairment of autophagy and increased oxidative stress are involved in the development of kidney fibrosis and damage. Autophagy impairment inhibits the degradation of damaged cellular components and the regulation of profibrotic mediators such as TGF-β, leading to increased collagen accumulation, apoptosis of tubular epithelial cells, and the enhanced activity

of fibrogenic pathways (97, 98). Oxidative stress, caused by the overproduction of ROS, activates NADPH oxidase and downstream Smad-dependent signaling pathways, which in turn lead to excessive extracellular matrix deposition, apoptosis, and chronic inflammation (98, 99). These interrelated alterations create a cellular microenvironment for promoting how kidney injury and fibrosis progress. These results suggest that a normal autophagic process plays an essential role in reducing oxidative stress and limiting fibrotic processes. Injury to tubular cells may also affect autophagy, resulting in direct cell injury and the promotion of pro-fibrotic pathways (100). Together, these studies highlight the importance of restoring autophagy and decreasing oxidative stress in reducing NSAID-induced kidney injury and its progression to fibrosis, although the precise timing of NSAID-induced tubular injury and autophagy impairment remains to be determined (97, 99).
Although the results of this study are valuable, it is essential to consider that animal and laboratory models may not accurately represent human physiology and metabolism, and genetics may play a role in NSAID responses in humans (101). The number of subjects in the high-dose naproxen group, due to drug-induced enteropathy, was low, which could be viewed as a limitation; however, the results were statistically meaningful. A further limitation of our study is not having serum and urine chemistries available to assess renal retention parameters or proteinuria, but the renal histology of the rats in our study does not suggest an increase in retention. Future studies on NSAID nephrotoxicity may incorporate the use of more physiologically relevant models, as well as larger and more diverse animal populations. Other possibilities could involve the use of methods to protect against nephrotoxicity, including antioxidants or specific signaling pathway inhibitors. The use of newer technologies, such as organoids or 3D cultures, is another promising approach to elucidate the relationship between autophagy and fibrosis, as well as the development of preventive strategies for chronic kidney injury (102).

5.2 NSAID-Induced Enteropathy

We identified the changes in the expression of the main intestinal antimicrobial peptides (AMPs) and systemic hematological changes, and the resulting effects and interplays between them involved in the pathogenesis of indomethacin (IND)-induced enteropathy in rats. We demonstrated that the expression of the cathelicidin gene is upregulated in the small intestine in response to inflammatory injury induced by high-dose IND, and this upregulation is detectable as early as 12 h after IND administration. Furthermore, this increase was also positively correlated with the

expression of other proinflammatory cytokines IL-1b and TNF-α in the acute model, whereas cathelicidin is known as an inducible AMP whose expression is regulated by inflammation (103, 104). Beyond its direct antimicrobial activity, cathelicidin also has immunomodulatory properties through neutrophil recruitment and tissue repair (105, 106). The persistent cathelicidin up-regulation in the acute and chronic IND model suggests continuous natural immune stimulation in inflamed mucosa, thus making the protein a potential biomarker for intestinal inflammatory activity. In contrast, the expression of α-defensin 5 (Defa5) and β-defensin 2 (Defb2) was much more variable, and there were no meaningful changes in the acute treatment. In the chronic administration, Defa5 was markedly upregulated in relation to higher IND dosing (4 mg/kg). Differences in results between the two studies suggest that the regulation of defensins in NSAID enteropathy may be modified by duration of injury and adaptation mechanisms. Upregulation of Defa5 in chronic injury could be a compensatory epithelial response or could reflect changes in gut microbiota composition over time, since some bacteria-derived metabolites can induce defensin gene expression (107, 108). This finding contrasts with some previous reports of defensin deficiency in acute injury (109, 110), underscoring the complex role of AMPs in enteropathy.

We also noted the hematological changes of the chronic model with decrease of red blood cell indices, along with an increase of platelet-associated parameters, representing systemic effects of severe enteropathy. Decreased hemoglobin and hematocrit are highly suggestive of chronic occult blood loss from intestinal ulcers leading to iron deficiency anemia. At the same time, the observed platelet alterations may reflect a systemic inflammatory state that can impact hematopoiesis and platelet dynamics. The early onset of these hematological abnormalities shows their potential utility as indirect and systemic indicators of significant intestine injury.

In conclusion, our findings reveal a differential regulation of intestinal AMPs in the context of IND-induced enteropathy that involves an inflammation-responsive upregulation of cathelicidin and a distinct α-defensin (α-defensin 5) response that was considerably upregulated in chronic injury settings only. Associated blood abnormalities confirm the systemic dimensions of this drug-induced illness. This study mainly limits itself to male animals, and future studies should include females for examination of whether such differences exist in this model. Further studies are therefore necessary to understand the specific functional consequences of these AMP modifications on disease progression and mucosal repair, and to explore their relationship with long-term NSAID use. Eventually, understanding these patterns may contribute to the development novel monitoring

strategies or therapeutic approaches aimed at modifying the host antimicrobial response in NSAID enteropathy.

6 CONCLUSIONS

This thesis expands on our understanding of the underlying molecular mechanisms of NSAID-induced renal and intestinal injury, identifying pathways other than COX inhibition that may be targets for improved prevention and treatment. A significant methodological contribution is the discovery that culture medium has a substantial impact on TGF-β1-driven EMT and EGR1 activation in HK-2 cells. By choosing DMEM with 5% FBS as the most precise and reproducible condition, we address a fundamental distracting factor in preclinical renal research, thereby providing greater reliability in connecting in vitro findings with in vivo and clinical reality. In NSAID-induced nephrotoxicity, high-dose celecoxib and naproxen inhibit tubular function in vivo through COX-independent mechanisms, including the inhibition of autophagy, oxidative stress, and EGR1-dependent profibrotic signaling in tubular cells. These COX-independent effects highlight autophagy dysfunction and EGR1 as central mediators, suggesting that selective NSAIDs may pose greater renal risks in vulnerable patients than previously appreciated. In addition to this, indomethacin-induced enteropathy contains inflammation-driven Cathelicidin overexpression and context-dependent defensin responses, along with systemic hematological markers of injury. This indicates impaired host-microbial defenses as a significant aspect of mucosal pathology.

Taken together, these results indicate that autophagy, oxidative stress, EGR1 signaling and antimicrobial peptides all play a role in NSAID toxicity, suggesting new strategies for treating CKD and enteropathy. Clinically, they support the consideration of NSAID use and dose adjustment and monitoring in high-risk populations. Therapeutically, rescue of autophagy, inhibition of EGR1, and manipulation of AMP levels can help to reduce the injury and preserve organ function.

Novelty of the Thesis:

- We have identified cell culture medium formulation as one of the determinants of the reproducibility of EMT in HK-2 cells, solving a major issue in kidney fibrosis modeling.
- We have elucidated COX-independent mechanisms by which high-dose celecoxib and naproxen induce autophagy impairment, oxidative stress, and EGR1-mediated renal fibrosis using integrated *in vitro* and *in vivo* models.
- We have described differential regulation of antimicrobial peptides and systemic biomarkers in NSAID enteropathy, offering new biomarkers and insights into host defense dysfunction.

7 SUMMARY

Nonsteroidal anti-inflammatories (NSAIDs) are among the most widely used medications in the world for the treatment of pain and inflammation. High-dose NSAID use or long-term NSAID use is associated with significant renal and gastrointestinal toxicities, often through mechanisms independent of cyclooxygenase (COX) inhibition. Chronic kidney disease (CKD) is one of the major burdens on the globe's health systems. Tubulointerstitial renal fibrosis is the end-stage for CKD. NSAID-induced small intestinal enteropathy is a well-known side effect of NSAID use that is under-recognized. This thesis elucidates the molecular mechanisms underlying NSAID-associated enteropathy, employing an integrated in vitro and in vivo approach to uncover novel pathways.

To find an appropriate preclinical model, we optimized the culture conditions for TGF-β1-induced EMT in HK-2 cells. TGF-β1-induced EMT of HK-2 cells was optimized in DMEM 5% FBS culture medium, which led to the most significant response to the TGFB1-EGR1 interaction. This was a breakthrough in eliminating the major source of variability affecting the results of studies related to renal fibrosis-related diseases.

In NSAID renal injury models, high-dose celecoxib and naproxen (but not indomethacin) have been associated with direct tubular epithelial toxicity, upregulation of pro-fibrotic and autophagic genes, decreased autophagic flux, and oxidative stress responses, both in vitro and in rat renal medulla, leading to mild structural alterations via COX-independent mechanisms.

In rats with NSAID-induced enteropathy, indomethacin altered the expression of small intestinal antimicrobial peptides, with cathelicidin uniformly upregulated due to inflammation and defensins altered in a phase-dependent changes. Systemic hematological changes also revealed evidence of mucosal damage and inflammation.

These data support COX-independent mechanisms of NSAID toxicity, including impaired autophagy, oxidative stress, EGR1-mediated signaling of kidney injury and fibrosis, and altered host defense in the intestine. Therefore, NSAIDs should be used with caution in patients at risk of nephrotoxicity and enteropathy. The data provides potential targets for reducing associated organ injury and the treatment of CKD.

8 RFERENCES

1. Glassock RJ, Winearls C. The global burden of chronic kidney disease: how valid are the estimates? Nephron Clin Pract. 2008;110(1):39-47.

2. Wongrakpanich S, Wongrakpanich A, Melhado K, Rangaswami J. A Comprehensive Review of Non-Steroidal Anti-Inflammatory Drug Use in The Elderly. Aging Dis. 2018;9(1):143-50.

3. Conaghan PG. A turbulent decade for NSAIDs: update on current concepts of classification, epidemiology, comparative efficacy, and toxicity. Rheumatol Int. 2012;32(6):1491-502.

4. Vane JR, Botting RM. Mechanism of action of antiinflammatory drugs. Int J Tissue React. 1998;20(1):3-15.

5. Ricciotti E, FitzGerald GA. Prostaglandins and inflammation. Arterioscler Thromb Vasc Biol. 2011;31(5):986-1000.

6. Harirforoosh S, Asghar W, Jamali F. Adverse effects of nonsteroidal antiinflammatory drugs: an update of gastrointestinal, cardiovascular and renal complications. J Pharm Pharm Sci. 2013;16(5):821-47.

7. Bindu S, Mazumder S, Bandyopadhyay U. Non-steroidal anti-inflammatory drugs (NSAIDs) and organ damage: A current perspective. Biochem Pharmacol. 2020;180:114147.

8. Bjarnason I, Scarpignato C, Holmgren E, Olszewski M, Rainsford KD, Lanas A. Mechanisms of Damage to the Gastrointestinal Tract From Nonsteroidal Anti-Inflammatory Drugs. Gastroenterology. 2018;154(3):500-14.

9. Hörl WH. Nonsteroidal Anti-Inflammatory Drugs and the Kidney. Pharmaceuticals (Basel). 2010;3(7):2291-321.

10. Lucas GNC, Leitão ACC, Alencar RL, Xavier RMF, Daher EF, Silva Junior GBD. Pathophysiological aspects of nephropathy caused by non-steroidal anti-inflammatory drugs. J Bras Nefrol. 2019;41(1):124-30.

11. Maiden L, Thjodleifsson B, Theodors A, Gonzalez J, Bjarnason I. A quantitative analysis of NSAID-induced small bowel pathology by capsule enteroscopy. Gastroenterology. 2005;128(5):1172-8.

12. Vane JR, Botting RM. Mechanism of action of nonsteroidal anti-inflammatory drugs. Am J Med. 1998;104(3a):2S-8S; discussion 21S-2S.

13. Tune BM, Fravert D. Mechanisms of cephalosporin nephrotoxicity: a comparison of cephaloridine and cephaloglycin. Kidney Int. 1980;18(5):591-600.
14. Whelton A. Nephrotoxicity of nonsteroidal anti-inflammatory drugs: physiologic foundations and clinical implications. Am J Med. 1999;106(5b):13s-24s.
15. Perazella MA, Tray K. Selective cyclooxygenase-2 inhibitors: a pattern of nephrotoxicity similar to traditional nonsteroidal anti-inflammatory drugs. Am J Med. 2001;111(1):64-7.
16. Komers R, Anderson S, Epstein M. Renal and cardiovascular effects of selective cyclooxygenase-2 inhibitors. Am J Kidney Dis. 2001;38(6):1145-57.
17. Djudjaj S, Boor P. Cellular and molecular mechanisms of kidney fibrosis. Mol Aspects Med. 2019;65:16-36.
18. Bülow RD, Boor P. Extracellular Matrix in Kidney Fibrosis: More Than Just a Scaffold. J Histochem Cytochem. 2019;67(9):643-61.
19. Gewin LS. Renal fibrosis: Primacy of the proximal tubule. Matrix Biol. 2018;68-69:248-62.
20. Edeling M, Ragi G, Huang S, Pavenstädt H, Susztak K. Developmental signalling pathways in renal fibrosis: the roles of Notch, Wnt and Hedgehog. Nat Rev Nephrol. 2016;12(7):426-39.
21. Meng XM, Nikolic-Paterson DJ, Lan HY. TGF-β: the master regulator of fibrosis. Nat Rev Nephrol. 2016;12(6):325-38.
22. Ma T-T, Meng X-M. TGF-β/Smad and Renal Fibrosis. In: Liu B-C, Lan H-Y, Lv L-L, editors. Renal Fibrosis: Mechanisms and Therapies. Singapore: Springer Singapore; 2019. p. 347-64.
23. Böttinger EP, Bitzer M. TGF-beta signaling in renal disease. J Am Soc Nephrol. 2002;13(10):2600-10.
24. López-Hernández FJ, López-Novoa JM. Role of TGF-β in chronic kidney disease: an integration of tubular, glomerular and vascular effects. Cell Tissue Res. 2012;347(1):141-54.
25. Meng XM, Nikolic-Paterson DJ, Lan HY. TGF-β: the master regulator of fibrosis. Nat Rev Nephrol. 2016;12(6):325-38.
26. Shen L, Yin H, Sun L, Zhang Z, Jin Y, Cao S. Iguratimod attenuated fibrosis in systemic sclerosis via targeting early growth response 1 expression. Arthritis Res Ther. 2023;25(1):151.

27. Xie Y, Li Y, Chen J, Ding H, Zhang X. Early growth response-1: Key mediators of cell death and novel targets for cardiovascular disease therapy. Front Cardiovasc Med. 2023;10:1162662.
28. Bhattacharyya S, Wu M, Fang F, Tourtellotte W, Feghali-Bostwick C, Varga J. Early growth response transcription factors: key mediators of fibrosis and novel targets for anti-fibrotic therapy. Matrix Biol. 2011;30(4):235-42.
29. Chen SJ, Ning H, Ishida W, Sodin-Semrl S, Takagawa S, Mori Y. The early-immediate gene EGR-1 is induced by transforming growth factor-β and mediates stimulation of collagen gene expression. J Biol Chem. 2006;281(30):21183-97.
30. Bhattacharyya S, Fang F, Tourtellotte W, Varga J. Egr-1: new conductor for the tissue repair orchestra directs harmony (regeneration) or cacophony (fibrosis). J Pathol. 2013;229(2):286-97.
31. Chen J, Chen Y, Olivero A, Chen X. Identification and validation of potential biomarkers and their functions in acute kidney injury. Front Genet. 2020;11:411.
32. Jeong K, Je J, Dusabimana T, Kim H, Park SW. Early Growth Response 1 Contributes to Renal IR Injury by Inducing Proximal Tubular Cell Apoptosis. Int J Mol Sci. 2023;24(18):14295.
33. Xu P, Zhan H, Zhang R, Xu XJ, Zhang Y, Le Y, Bi JG. Early growth response factor 1 upregulates pro-fibrotic genes through activation of TGF-β1/Smad pathway via transcriptional regulation of PAR1 in high-glucose treated HK-2 cells. Mol Cell Endocrinol. 2023;572:111953.
34. Carl M, Akagi Y, Weidner S, Isaka Y, Imai E, Rupprecht HD. Specific inhibition of Egr-1 prevents mesangial cell hypercellularity in experimental nephritis. Kidney Int. 2003;63(4):1302-12.
35. Yang YL, Hu F, Xue M, Jia YJ, Zheng ZJ, Li Y, Xue YM. Early growth response protein-1 upregulates long noncoding RNA Arid2-IR to promote extracellular matrix production in diabetic kidney disease. Am J Physiol Cell Physiol. 2019;316(3):C340-c52.
36. Nakamura H, Isaka Y, Tsujie M, Rupprecht H, Akagi Y, Ueda N. Introduction of DNA enzyme for Egr-1 into tubulointerstitial fibroblasts by electroporation reduced interstitial α-smooth muscle actin expression and fibrosis in unilateral ureteral obstruction (UUO) rats. Gene Ther. 2002;9(8):495-502.
37. Agras PI, Derbent M, Ozcay F, Baskin E, Turkoglu S, Aldemir D. Effect of congenital heart disease on renal function in childhood. Nephron Physiol. 2005;99(1):10-5.

38. Gómez-Lechón MJ, Ponsoda X, O'Connor E, Donato T, Castell JV, Jover R. Diclofenac induces apoptosis in hepatocytes by alteration of mitochondrial function and generation of ROS. Biochem Pharmacol. 2003;66(11):2155-67.
39. Abraham NG, Kappas A. Pharmacological and clinical aspects of heme oxygenase. Pharmacol Rev. 2008;60(1):79-127.
40. László SB, Hutka B, Tóth AS, Hegyes T, Demeter ZO, Haghighi A. Celecoxib and rofecoxib have different effects on small intestinal ischemia/reperfusion injury in rats. Front Pharmacol. 2024;15:1468579.
41. Cantley LC. The phosphoinositide 3-kinase pathway. Science. 2002;296(5573):1655-7.
42. Brazil DP, Yang ZZ, Hemmings BA. Advances in protein kinase B signalling: AKTion on multiple fronts. Trends Biochem Sci. 2004;29(5):233-42.
43. Tang C, Livingston MJ, Liu Z, Dong Z. Autophagy in kidney homeostasis and disease. Nat Rev Nephrol. 2020;16(9):489-508.
44. Kimura T, Takabatake Y, Takahashi A, Kaimori JY, Matsui I, Namba T. Autophagy protects the proximal tubule from degeneration and acute ischemic injury. J Am Soc Nephrol. 2011;22(5):902-13.
45. Sang J, Zhang K, Fan Q, Kan C, Pan R, Sun X, Guo Z. Autophagy-senescence interplay in kidney disease: mechanistic insights and therapeutic potential. Mol Biol Rep. 2025;53(1):22.
46. Yang X, Wang H, Tu Y, Li Y, Zou Y, Li G. WNT1-inducible signaling protein-1 mediates TGF-β1-induced renal fibrosis in tubular epithelial cells and unilateral ureteral obstruction mouse models via autophagy. J Cell Physiol. 2020;235(3):2009-22.
47. Kaushal GP, Chandrashekar K, Juncos LA, Shah SV. Autophagy function and regulation in kidney disease. Biomolecules. 2020;10(1):100.
48. Huber TB, Edelstein CL, Hartleben B, Inoki K, Jiang M, Koya D. Emerging role of autophagy in kidney function, diseases and aging. Autophagy. 2012;8(7):1009-31.
49. Sureshbabu A, Muhsin SA, Choi ME. TGF-β signaling in the kidney: profibrotic and protective effects. Am J Physiol Renal Physiol. 2016;310(7):F596-F606.
50. Guo S, Al-Sadi R, Said HM, Ma TY. Lipopolysaccharide causes an increase in intestinal tight junction permeability in vitro and in vivo by inducing enterocyte membrane expression and localization of TLR-4 and CD14. Am J Pathol. 2013;182(2):375-87.

51. Zoetendal EG, Raes J, van den Bogert B, Arumugam M, Booijink CC, Troost FJ, Bork P, Wels M, de Vos WM, Kleerebezem M. The human small intestinal microbiota is driven by rapid uptake and conversion of simple carbohydrates. Isme j. 2012;6(7):1415-26.
52. Mansour B, Monyók Á, Makra N, Gajdács M, Vadnay I, Ligeti B, Juhász J, Szabó D, Ostorhazi OE. Bladder cancer-related microbiota: examining differences in urine and tissue samples. Sci Rep. 2020;10(1):11042.
53. Wood DE, SL S. Kraken: ultrafast metagenomic sequence classification using exact alignments. Genome biology. 2014;15(3):R46.
54. Bolger AM, Lohse M, Usadel B. Trimmomatic: a flexible trimmer for Illumina sequence data. Bioinformatics. 2014;30(15):2114-20.
55. Haghighi A, Tóth AS, Demeter ZO, Hutka B, Zsidai A, Lengyel L, Haghighi S, Pannier M, Le Cosquer G, Meunier ES, Ágg B, Makra N, Ostorházi E, Ligeti B, Kovács K, Kelemen Á, Jakab A, Wachtl G, Kökény G, Szabó D, Ferdinandy P, Motta JP, Vergnolle N, Gyires K, Zádori ZS. Oral indomethacin modifies small intestine biofilms and host-microbe interaction mediators. Life Sci. 2026;384:124114.
56. Blackler RW, Gemici B, Manko A, Wallace JL. NSAID-gastroenteropathy: new aspects of pathogenesis and prevention. Curr Opin Pharmacol. 2014;19:11-6.
57. Bevins CL, Salzman NH. Paneth cells, antimicrobial peptides and maintenance of intestinal homeostasis. Nat Rev Microbiol. 2011;9(5):356-68.
58. Higuchi K, Umegaki E, Watanabe T, Yoda Y, Morita E, Murano M, Tokioka S, Arakawa T. Present status and strategy of NSAIDs-induced small bowel injury. J Gastroenterol. 2009;44(9):879-88.
59. Niederberger E, Tegeder I, Vetter G, Schmidtko A, Schmidt H, Euchenhofer C, Bräutigam L, Grösch S, Geisslinger G. Celecoxib loses its anti-inflammatory efficacy at high doses through activation of NF-kappaB. Faseb j. 2001;15(9):1622-4.
60. Dahan A, Duvdevani R, Dvir E, Elmann A, Hoffman A. A novel mechanism for oral controlled release of drugs by continuous degradation of a phospholipid prodrug along the intestine: in-vivo and in-vitro evaluation of an indomethacin-lecithin conjugate. J Control Release. 2007;119(1):86-93.
61. Davies NM, Anderson KE. Clinical pharmacokinetics of naproxen. Clin Pharmacokinet. 1997;32(4):268-93.

62. Reagan-Shaw S, Nihal M, Ahmad N. Dose translation from animal to human studies revisited. Faseb j. 2008;22(3):659-61.
63. Garmaa G, Manzéger A, Haghighi S, Kökény G. HK-2 cell response to TGF-β highly depends on cell culture medium formulations. Histochem Cell Biol. 2024;161(1):69-79.
64. Haghighi S, Haghighi A, Zádori ZS, Kovács K, Manzéger A, Kökény GJE, Pathology M. Celecoxib and naproxen disrupt autophagy and activate EGR1 in kidney tubules. 2025;144:105000.
65. Baker M, Perazella MA. NSAIDs in CKD: are they safe? American Journal of Kidney Diseases. 2020;76(4):546-57.
66. Klionsky DJ, Abdalla FC, Abeliovich H, Abraham RT, Acevedo-Arozena A, Adeli K, Agholme L, Klimecki WT, Klucken J, Knecht E, Ko BC, Koch JC, Koga H, Koh JY, Koh YH, Koike M, Komatsu M, Kominami E, Tsung A. Guidelines for the use and interpretation of assays for monitoring autophagy. Autophagy. 2012;8(4):445-544.
67. Hirakawa Y, Tanaka T, Nangaku M. Renal Hypoxia in CKD; Pathophysiology and Detecting Methods. Front Physiol. 2017;8:99.
68. Mózes MM, Szoleczky P, Rosivall L, Kökény G. Sustained hyperosmolarity increses TGF-ß1 and Egr-1 expression in the rat renal medulla. BMC Nephrol. 2017;18(1):209.
69. Whelton A, Schulman G, Wallemark C, Drower EJ, Isakson PC, Verburg KM, Geis GS. Effects of celecoxib and naproxen on renal function in the elderly. Arch Intern Med. 2000;160(10):1465-70.
70. Khan KNM, Alden CL, Gleissner SE, Gessford MK, Maziasz TJ. Effect of papillotoxic agents on expression of cyclooxygenase isoforms in the rat kidney. Toxicologic pathology. 1998;26(1):137-42.
71. Tegeder I, Pfeilschifter J, Geisslinger G. Cyclooxygenase-independent actions of cyclooxygenase inhibitors. The FASEB Journal. 2001;15(12):2057-72.
72. Nehus E, Kaddourah A, Bennett M, Pyles O, Devarajan P. Subclinical kidney injury in children receiving nonsteroidal anti-inflammatory drugs after cardiac surgery. The Journal of pediatrics. 2017;189:175-80.
73. Obeid S, Libby P, Husni E, Wang Q, Wisniewski LM, Davey DA, Wolski KE, Xia F, Bao W, Walker C. Cardiorenal risk of celecoxib compared with naproxen or ibuprofen in arthritis patients: insights from the PRECISION trial. European Heart Journal-Cardiovascular Pharmacotherapy. 2022;8(6):611-21.

74. Scharenberg MA, Pippenger BE, Sack R, Zingg D, Ferralli J, Schenk S, Martin I, Chiquet-Ehrismann R. TGF-β-induced differentiation into myofibroblasts involves specific regulation of two MKL1 isoforms. Journal of cell science. 2014;127(5):1079-91.
75. Kökény G, Németh Á, Kopp JB, Chen W, Oler AJ, Manzéger A, Rosivall L, Mózes MM. Susceptibility to kidney fibrosis in mice is associated with early growth response-2 protein and tissue inhibitor of metalloproteinase-1 expression. Kidney international. 2022;102(2):337-54.
76. Fang F, Ooka K, Bhattachyya S, Wei J, Wu M, Du P, Lin S, Del Galdo F, Feghali-Bostwick CA, Varga J. The early growth response gene Egr2 (Alias Krox20) is a novel transcriptional target of transforming growth factor-β that is up-regulated in systemic sclerosis and mediates profibrotic responses. The American journal of pathology. 2011;178(5):2077-90.
77. Mózes MM, Szoleczky P, Rosivall L, Kökény G. Sustained hyperosmolarity increses TGF-ss1 and Egr-1 expression in the rat renal medulla. BMC nephrology. 2017;18(1):209.
78. Chen Z-H, Kim HP, Sciurba FC, Lee S-J, Feghali-Bostwick C, Stolz DB, Dhir R, Landreneau RJ, Schuchert MJ, Yousem SA. Egr-1 regulates autophagy in cigarette smoke-induced chronic obstructive pulmonary disease. PloS one. 2008;3(10):e3316.
79. Hao C-M, Yull F, Blackwell T, Kömhoff M, Davis LS, Breyer MD. Dehydration activates an NF-κB–driven, COX2-dependent survival mechanism in renal medullary interstitial cells. The Journal of clinical investigation. 2000;106(8):973-82.
80. Chun K-S, Kim S-H, Song Y-S, Surh Y-J. Celecoxib inhibits phorbol ester-induced expression of COX-2 and activation of AP-1 and p38 MAP kinase in mouse skin. Carcinogenesis. 2004;25(5):713-22.
81. Wei K-C, Lin J-T, Lin C-H. Celecoxib paradoxically induces COX-2 expression and astrocyte activation through the ERK/JNK/AP-1 signaling pathway in the cerebral cortex of rats. Neurochemistry International. 2025;183:105926.
82. Okabe M, Koike K, Yamamoto I, Tsuboi N, Matsusaka T, Yokoo T. Early growth response 1 as a podocyte injury marker in human glomerular diseases. Clinical Kidney Journal. 2024;17(1):sfad289.
83. Sanchez AP, Sharma K. Transcription factors in the pathogenesis of diabetic nephropathy. Expert reviews in molecular medicine. 2009;11:e13.

84. Kim S, Lee W, Cho K. P62 Links the Autophagy Pathway and the Ubiquitin–Proteasome System in Endothelial Cells during Atherosclerosis. International journal of molecular sciences. 2021;22(15):7791.
85. Yun HR, Jo YH, Kim J, Shin Y, Kim SS, Choi TG. Roles of autophagy in oxidative stress. International journal of molecular sciences. 2020;21(9):3289.
86. Hennig P, Fenini G, Di Filippo M, Karakaya T, Beer H-D. The pathways underlying the multiple roles of p62 in inflammation and cancer. Biomedicines. 2021;9(7):707.
87. Ding Y, ll Kim S, Lee S-Y, Koo JK, Wang Z, Choi ME. Autophagy regulates TGF-β expression and suppresses kidney fibrosis induced by unilateral ureteral obstruction. Journal of the American Society of Nephrology. 2014;25(12):2835-46.
88. Kim SI, Na H-J, Ding Y, Wang Z, Lee SJ, Choi ME. Autophagy promotes intracellular degradation of type I collagen induced by transforming growth factor (TGF)-β1. Journal of Biological Chemistry. 2012;287(15):11677-88.
89. Kitada M, Takeda A, Nagai T, Ito H, Kanasaki K, Koya D. Dietary restriction ameliorates diabetic nephropathy through anti-inflammatory effects and regulation of the autophagy via restoration of Sirt1 in diabetic Wistar fatty (fa/fa) rats: A model of type 2 diabetes. Journal of Diabetes Research. 2011;2011(1):908185.
90. Vallon V, Rose M, Gerasimova M, Satriano J, Platt KA, Koepsell H, Cunard R, Sharma K, Thomson SC, Rieg T. Knockout of Na-glucose transporter SGLT2 attenuates hyperglycemia and glomerular hyperfiltration but not kidney growth or injury in diabetes mellitus. American Journal of Physiology-Renal Physiology. 2013;304(2):F156-F67.
91. Yamahara K, Kume S, Koya D, Tanaka Y, Morita Y, Chin-Kanasaki M, Araki H, Isshiki K, Araki S-i, Haneda M. Obesity-mediated autophagy insufficiency exacerbates proteinuria-induced tubulointerstitial lesions. Journal of the American Society of Nephrology. 2013;24(11):1769-81.
92. Liu R, Zhang X, Nie L, Sun S, Liu J, Chen H. Heme oxygenase 1 in erythropoiesis: an important regulator beyond catalyzing heme catabolism. Ann Hematol. 2023;102(6):1323-32.
93. Wiener CM, Booth G, Semenza GL. In vivoexpression of mRNAs encoding hypoxia-inducible factor 1. Biochemical and biophysical research communications. 1996;225(2):485-8.
94. Hou CC, Hung SL, Kao SH, Chen TH, Lee HM. Celecoxib induces heme-oxygenase expression in glomerular mesangial cells. Ann N Y Acad Sci. 2005;1042:235-45.

95. Cantoni L, Valaperta R, Ponsoda X, Castell JV, Barelli D, Rizzardini M, Mangolini A, Hauri L, Villa P. Induction of hepatic heme oxygenase-1 by diclofenac in rodents: role of oxidative stress and cytochrome P-450 activity. J Hepatol. 2003;38(6):776-83.
96. HOU CC, HUNG SL, KAO SH, Chen TH, LEE HM. Celecoxib induces heme-oxygenase expression in glomerular mesangial cells. Annals of the New York Academy of Sciences. 2005;1042(1):235-45.
97. Manzéger A, Garmaa G, Mózes MM, Hansmann G, Kökény G. Pioglitazone Protects Tubular Epithelial Cells during Kidney Fibrosis by Attenuating miRNA Dysregulation and Autophagy Dysfunction Induced by TGF-β. Int J Mol Sci. 2023;24(21).
98. Ruart M, Chavarria L, Campreciós G, Suárez-Herrera N, Montironi C, Guixé-Muntet S, Bosch J, Friedman SL, Garcia-Pagán JC, Hernández-Gea V. Impaired endothelial autophagy promotes liver fibrosis by aggravating the oxidative stress response during acute liver injury. J Hepatol. 2019;70(3):458-69.
99. Lv W, Booz GW, Fan F, Wang Y, Roman RJ. Oxidative Stress and Renal Fibrosis: Recent Insights for the Development of Novel Therapeutic Strategies. Front Physiol. 2018;9:105.
100. Livingston MJ, Zhang M, Kwon S-H, Chen J-K, Li H, Manicassamy S, Dong Z. Autophagy activates EGR1 via MAPK/ERK to induce FGF2 in renal tubular cells for fibroblast activation and fibrosis during maladaptive kidney repair. Autophagy. 2024;20(5):1032-53.
101. Becker GJ, Hewitson TD. Animal models of chronic kidney disease: useful but not perfect. Nephrol Dial Transplant. 2013;28(10):2432-8.
102. Dewhurst RM, Molinari E, Sayer JAJM, Nanofluidics. Spheroids, organoids and kidneys-on-chips: how complex human cellular models have assisted in the study of kidney disease and renal ciliopathies. 2023;27(3):21.
103. Koon HW, Shih DQ, Chen J, Bakirtzi K, Hing TC, Law I, Ho S, Ichikawa R, Zhao D, Xu XH. Cathelicidin signaling via the Toll-like receptor protects against colitis in mice. Gastroenterology. 2011;141(5):1852-63. e3.
104. Hutka B, Várallyay A, László SB, Tóth AS, Scheich B, Paku S, Vörös I, Pós Z, Varga ZV, Norman D. A dual role of lysophosphatidic acid type 2 receptor (LPAR2) in nonsteroidal anti-inflammatory drug-induced mouse enteropathy. Acta Pharmacologica Sinica. 2024;45(2):339-53.
105. Rivas-Santiago B, Hernandez-Pando R, Carranza C, Juarez E, Contreras JL, Aguilar-Leon D, Torres M, Sada EJI, immunity. Expression of cathelicidin LL-37 during Mycobacterium

tuberculosis infection in human alveolar macrophages, monocytes, neutrophils, and epithelial cells. 2008;76(3):935-41.

106. Höpfinger A, Karrasch T, Schäffler A, Schmid A. Regulation of CAMP (cathelicidin antimicrobial peptide) expression in adipocytes by TLR 2 and 4. Innate Immun. 2021;27(2):184-91.

107. Sugi Y, Takahashi K, Kurihara K, Nakano K, Kobayakawa T, Nakata K, Tsuda M, Hanazawa S, Hosono A, Kaminogawa S. α-Defensin 5 gene expression is regulated by gut microbial metabolites. Biosci Biotechnol Biochem. 2017;81(2):242-8.

108. Takakuwa A, Nakamura K, Kikuchi M, Sugimoto R, Ohira S, Yokoi Y, Ayabe T. Butyric Acid and Leucine Induce α-Defensin Secretion from Small Intestinal Paneth Cells. Nutrients. 2019;11(11).

109. Tanigawa T, Watanabe T, Otani K, Nadatani Y, Ohkawa F, Sogawa M, Yamagami H, Shiba M, Watanabe K, Tominaga K, Fujiwara Y, Takeuchi K, Arakawa T. Rebamipide inhibits indomethacin-induced small intestinal injury: possible involvement of intestinal microbiota modulation by upregulation of α-defensin 5. Eur J Pharmacol. 2013;704(1-3):64-9.

110. Chamoun-Emanuelli AM, Bryan LK, Cohen ND, Tetrault TL, Szule JA, Barhoumi R, Whitfield-Cargile CM. NSAIDs disrupt intestinal homeostasis by suppressing macroautophagy in intestinal epithelial cells. Sci Rep. 2019;9(1):14534.

9 PUBLICATION

Publications related to the thesis:

1. Haghighi S, Haghighi A, Zádori ZS, Kovács K, Manzéger A, Kökény G. Celecoxib and naproxen disrupt autophagy and activate EGR1 in kidney tubules. Experimental and Molecular Pathology. 2025;144:105000. Impact factor, journal quartile – 3.7, Q1.
2. Garmaa G, Manzéger A, **Haghighi S**, Kökény G. HK-2 cell response to TGF-β highly depends on cell culture medium formulations. Histochemistry and Cell Biology. 2024;161(1):69-79. Impact factor, journal quartile – 2.1, Q1.
3. Haghighi A, Tóth AS, Demeter ZO, Hutka B, Zsidai A, Lengyel L, **Haghighi S**, Pannier M, Le Cosquer G, Meunier ES, Ágg B, Makra N, Ostorházi E, Ligeti B, Kovács K, Kelemen Á, Jakab A, Wachtl G, Kökény G, Szabó D, Zádori ZS. Oral indomethacin modifies small intestine biofilms and host-microbe interaction mediators. Life Sciences. 2025;384:124114. Impact factor, journal quartile – 5.1, D1.

Publications not related to the thesis:

1. Haghighi Bardineh SA, Balou HA, Sedigh Ebrahim-Saraie H, Mobayen M, Esmailzadeh M, **Haghighi S**, Haghighi A, Sadeghi M. Predictive value of serum albumin and calcium levels in burn patients with Pseudomonas aeruginosa infection: A comprehensive analysis of clinical outcomes. International Wound Journal. 2024;21(3):14786. Impact factor, journal quartile – 2.5, Q1.
2. Salehi Z, Haghighi A, **Haghighi S**, Aminian K, Asl SF, Mashayekhi F. Mitochondrial DNA Deletion Δ4977 in Peptic Ulcer Disease. Molecular Biology. 2017;51(1):30-33. Impact factor, journal quartile – 0.977, Q3.

10 ACKNOWLEDGEMENTS

First and foremost, I would like to express my deepest gratitude to my supervisor, **Dr. Gábor Kökény**. His continuous guidance, scientific insight, patience, and unwavering support have been the foundation of this work and have taught me invaluable lessons throughout my PhD journey.

I am sincerely grateful to **Prof. Zoltán Benyó**, Program Director of the Pathophysiology and Translational Medicine Program, for his generous and tireless support, insightful advice, and for giving me the opportunity to conduct my research at Semmelweis University.

My special thanks go to the **Renal Fibrosis Research Group** and the **Institute of Clinical Pathophysiology**, as well as to **Dr. Anna Manzéger** and **Dr. Gantsetseg Garmaa** for their dedicated help, excellent collaboration, and constant encouragement during the experimental work.

I would like to thank the entire team at the Institute of Pharmacology and Pharmacotherapy for the friendly and supportive working environment, with special gratitude to **Dr. Zoltán S. Zádori** and my sister **Arezoo Haghighi** for their endless support, countless hours of help, and invaluable contributions that made this thesis possible.

Finally, I would like to express my heartfelt appreciation to my family — **my parents (Seyed Gholamreza and Seyyedeh Ghoncheh)**, my sister **Arzoo**, and my brother **Omid** — for their endless love, encouragement, and sacrifices that made this journey possible.

This work was financially supported by the **Stipendium Hungaricum**, the **SE250+ Excellence PhD Scholarship**, and the **National Research, Development and Innovation Office, Hungary (NKFI FK138842) Predoctoral Scholarship**.